Molecular Phylogenetics and Evolution 204 (2025) 108275

Contents lists available at ScienceDirect

Molecular Phylogenetics and Evolution

journal homepage: www.elsevier.com/locate/ympev

Phylogenetics, biogeography, and life history evolution in the broadly distributed treefrog genus *Dendropsophus* (Anura: Hylidae: Hylinae)

Courtney Whitcher [a,1,*], Victor G.D. Orrico [b,1], Santiago Ron [c], Mariana L. Lyra [d,e], Carla S. Cassini [f], Rodrigo B. Ferreira [g], Daniel Y.M. Nakamura [h], Pedro L.V. Peloso [i], Marco A. Rada [h], Mauricio Rivera-Correa [j,k], Marcelo J. Sturaro [l], Paula H. Valdujo [m], Célio F.B. Haddad [d], Taran Grant [h], Julian Faivovich [n,o], Alan Lemmon [p], Emily Moriarty Lemmon [q]

[a] *Florida State University, Department of Biological Science, Tallahassee, FL, USA*
[b] *Universidade Estadual de Santa Cruz, Departamento de Ciências Biológicas, Programa de Pós-Graduação em Zoologia, Brazil*
[c] *Museo de Zoología, Escuela de Biología, Facultad de Ciencias Exactas y Naturales, Pontificia Universidad Católica del Ecuador, 12 de Octubre y Roca, Quito, Ecuador*
[d] *Departamento de Biodiversidade and Centro de Aquicultura (CAUNESP), Instituto de Biociências, Universidade Estadual Paulista, Avenida 24 A 1515, C.P. 199, Rio Claro, SP, Brazil*
[e] *New York University Abu Dhabi, Saadiyat Island, Abu Dhabi, P.O. Box 129188, United Arab Emirates*
[f] *Departamento de Ciências Naturais, Universidade Estadual do Sudoeste da Bahia - Campus Itapetinga, BA, Brazil*
[g] *Programa de Pós-Graduação em Biologia Animal, (PPGBAN), Universidade Federal do Espírito Santo, Vitória, ES, Brazil*
[h] *Universidade de São Paulo, Departamento de Zoologia, São Paulo, Brazil*
[i] *California State University, Cal Poly Humboldt, Department of Biological Sciences, Arcata, CA, USA*
[j] *Laboratorio de Anfibios, Instituto de Ciencias Naturales, Universidad Nacional de Colombia, Bogotá, Colombia*
[k] *Grupo Herpetológico de Antioquia, Instituto de Biología, Universidad de Antioquia, Medellín, Colombia*
[l] *Universidade Federal de São Paulo, Diadema, Brazil*
[m] *The Biodiversity Consultancy, 3E Kings Parade CB2 1SJ, Cambridge, UK*
[n] *División Herpetología, Museo Argentino de Ciencias Naturales "Bernardino Rivadavia" –CONICET, Buenos Aires, Argentina*
[o] *Departamento de Biodiversidad y Biología Experimental, Facultad de Ciencias Exactas y Naturales, Universidad de Buenos Aires, Buenos Aires, Argentina*
[p] *Florida State University, Department of Scientific Computing, Center for Anchored Phylogenomics, Tallahassee, FL, USA*
[q] *Florida State University, Department of Biological Science, Center for Anchored Phylogenomics, Tallahssee, FL, USA*

A R T I C L E I N F O

Keywords:
Amphibian
Biogeography
Comparative methods
Neotropical
Phylogenetics

A B S T R A C T

Dendropsophus is one of the most species-rich genera of hylid treefrogs. Recent studies integrating Sanger-generated mitochondrial and nuclear loci with phenomic characters (SP) have advanced understanding of this clade, but questions about its internal relationships and biogeographic history persist. To address these questions, we used anchored hybrid enrichment (AHE) to combine 432 nuclear loci for 78 taxa (72 % of species) with published data. Quantitatively, the impact of the AHE data was modest, with compositional differences in only three recognized clades and more than 80 % of the clades in the AHE + SP analyses also supported in the SP-only analyses. Nevertheless, the impact of AHE was crucial for resolving and increasing support for multiple nodes. We transferred one species of the former *D. ruschii* group to the *D. decipiens* group and redefined the *D. leucophyllatus* group to avoid paraphyly. We estimated divergence times to reconstruct the clade's biogeographic history. We also examined evolution of oviposition sites and assessed its effect on lineage accumulation. *Dendropsophus* likely originated ~ 57 mya, predating the Andean uplift, with some taxa showing dispersal patterns less constrained by ecological changes than previously thought.

* Corresponding author at: Department of Biological Science, Florida State University, 319 Stadium Drive, Tallahassee, FL 32306 USA.
E-mail addresses: cwhitcher@bio.fsu.edu (C. Whitcher), vgdorrico@uesc.br (V.G.D. Orrico), marillyra@gmail.com (M.L. Lyra), carla.cassini@uesb.edu.br (C.S. Cassini), dani_ymn@usp.br (D.Y.M. Nakamura), pedropeloso@gmail.com (P.L.V. Peloso), radamarco@gmail.com (M.A. Rada), mauricio.rivera1@udea.edu.co (M. Rivera-Correa), marcelosturaro@gmail.com (M.J. Sturaro), paula.valdujo@thebiodiversityconsultancy.com (P.H. Valdujo), haddad1000@gmail.com (C.F.B. Haddad), taran.grant@ib.usp.br (T. Grant), jfaivovich@gmail.com (J. Faivovich).
[1] Indicates co-first authors.

https://doi.org/10.1016/j.ympev.2024.108275
Received 22 April 2024; Received in revised form 26 November 2024; Accepted 15 December 2024
Available online 24 December 2024

1. Introduction

The complex geological history of South and Central America has provided the impetus for multiple studies on the biogeographic history of the regions' amphibians (Heinicke et al., 2007, Elmer et al., 2013, Fouquet et al., 2014, Antonelli et al., 2018, Vasconcelos et al., 2019). Several studies point to an increase in cladogenesis among frogs during the late Miocene (approximately 13–8 mya; Gehara et al., 2014) as a consequence of increased environmental and elevational change during uplift of the Andes cordillera (Santos et al., 2009, Hoorn et al., 2010, Rohrmann et al., 2016; Rodriguez Tribaldos et al., 2017). Specifically, the regional climate changes caused by this uplift increased the influx of sediments both in the Amazon basin and offshore, fundamentally changing the Amazonian landscape by reconfiguring its drainage patterns (Hoorn et al., 2010) and correlated with evidence for Neogene uplift in the Atlantic Forest (Rodriguez Tribaldos et al., 2017). These geological and climatic changes multiplied the number of different habitat conditions, thus creating ecological opportunities for species to diversify (Hoorn et al., 2010), specifically within these changing regions.

Biogeographic studies have suggested up to five main routes for biotic interchange between Amazonia and the Atlantic Forest, which are major biotic regions in South America now separated by the Dry Diagonal (Fig. 1). Two of the five routes are thought to be the most probable connections between regions for amphibians (Batalha et al., 2013; Ledo and Colli, 2017; highlighted in Fig. 1). One passes through the northern Cerrado and Caatinga and represents a relatively young connection within the last 7 my (Batalha et al., 2013). A second older connection runs through modern Chaco to Bolivia and Paraguay, allowing dispersal prior to 23 mya (Batalha et al., 2013). Which of these routes was more important for amphibian dispersal is still being debated (Por, 1992; Oliveira et al., 1999; Batalha et al., 2013; Gehara et al., 2014). With 107 recognized species distributed from central Argentina to southern Mexico, *Dendropsophus* is one of the most diverse genera of hylid treefrogs (Frost, 2024). As such, it serves as an excellent model for biogeographic studies. Previous studies have examined the historical biogeography within species groups within *Dendropsophus* (Gehara et al., 2014; Pirani et al., 2020), but a comprehensive analysis of the historical dispersals across the genus has not been undertaken.

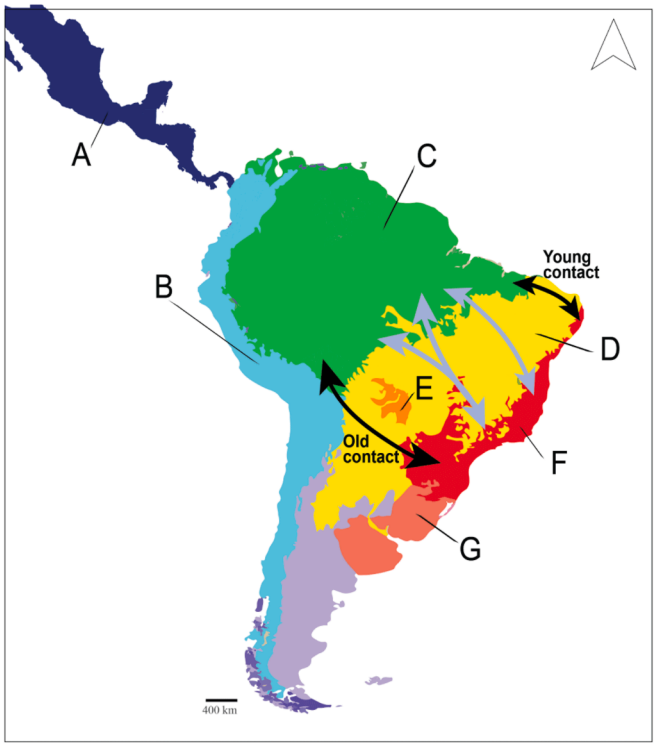

Fig. 1. Biomes of Central and South America used as character states for the ancestral state reconstruction of the geographic distributions of *Dendropsophus*; (A) Middle America, (B) Andes, (C) Amazonia, (D) Cerrado, Caatinga, and Chaco (The Dry Diagonal), (E) Pantanal, (F) Atlantic Forest, and (G) Pampas. Arrows denote five hypothesized routes of biotic interchange between Amazonia (C) and Atlantic Forest (G) as summarized in Ledo and Colli 2017 and Batalha-Filho et al. 2013. Black arrows represent the two most likely routes for amphibian dispersal as defined in Ledo and Colli 2017.

Additionally, species of *Dendropsophus* have two oviposition sites, aquatic and terrestrial (e.g., Bokermann, 1963; Duellman and Crump, 1974), with a few species having both modes (Touchon and Warkentin, 2008). Given that context-dependent selection appears to shape anuran reproductive phenotypes (Zamudio et al., 2016), it is possible that the shift to a different oviposition site and dispersal into new areas are related. Previous studies have suggested that oviposition plasticity may be an adaptation to new or variable mortality risks (Magnusson and Hero, 1991; Touchon and Warkentin, 2008; Touchon, 2012; Touchon and Worley, 2015). For example, Touchon and Worley (2015) found that *Dendrosophus ebraccatus* switches from aquatic to terrestrial oviposition when aquatic predators are present, suggesting that aquatic predation risk was a driver of the evolution of terrestrial reproduction. Alternatively, reproductive mode and oviposition site can be driven by intrasexual selection (Zamudio et al., 2016; de Sá et al., 2020). Specifically, terrestrial egg deposition is correlated with males hiding their mating behavior of amplexus from competing males (Zamudio et al., 2016) and a shift to smaller male body size (de Sa et al., 2020), two traits that release the male–male competition associated with exposed breeding. Finally, abiotic factors of temperature and humidity can constrain the evolution of terrestrial oviposition sites (Zamudio et al., 2016).

A well-resolved and supported phylogenetic hypothesis is needed to understand the biogeographic and life history diversification of *Dendropsophus*. The phylogenetic relationships within *Dendropsophus* were recently studied by Orrico et al. (2021) in a total-evidence analysis of eight genetic loci (three mitochondrial and five nuclear genes) and 201 phenomic (primarily internal and external morphological) characters. However, several regions of their topology lacked strong support, suggesting that additional data are needed to clarify the relationships within this group. In this study, we generated a novel dataset of 432 nuclear loci for 78 species (72 % of the genus) using anchored hybrid enrichment (AHE; Lemmon et al., 2012). To evaluate the impact of the new AHE data on understanding relationships among *Dendropsophus* species, we analyzed them both in isolation and together with data from Orrico et al. (2021) using both maximum likelihood and parsimony optimality criteria. Using divergence times estimated for the AHE dataset, we reconstructed the biogeographic history of the clade. Finally, we assessed the evolution of egg deposition site and examined correlations with lineage accumulation rate and the extent of biogeographic expansions.

2. Methods

2.1. Anchored hybrid enrichment (AHE) data collection

2.1.1. Sampling

We targeted 78 of the 107 recognized species of *Dendropsophus* (72 % of the genus), including two specimens for 15 % of the species (98 *Dendropsophus* terminals; Table S1-S2), for AHE. We also included 20 outgroup species, several with two individuals (27 outgroup terminals total; Table S1-S2), such that the full ingroup + outgroup AHE data set included 125 terminals.

2.1.2. Sequencing

We collected AHE data (Lemmon et al. 2012) through Florida State University's Center for Anchored Phylogenomics (https://www.anchoredphylogeny.com) following the protocol outlined in Prum et al.

(2015). We sonicated 1ug of extracted DNA to 200–400 bp using a Covaris Ultrasonicator on a 96-well glass plate. We prepared Illumina libraries following Meyer and Kircher (2010) on a Beckmann Coulter FXp Liquid handling robot, but with small modifications made by Prum et al. (2015). After pooling groups of ~ 16 samples with equal concentrations, we enriched the libraries using the AHE enrichment kit described by Hime et al. (2021). This amphibian-specific kit targets 364 nuclear loci. We pooled and sequenced the enriched libraries on an Illumina HiSeq2500 sequencer with a paired-end 200 bp protocol with one 8 bp indexing read. Sequencing was performed at Florida State University's College of Medicine Translational Lab. The total sequencing effort was 124.6 Gb (~1.2 Gb per sample).

2.1.3. AHE read assembly

Starting with the reads passing the Cassava high-chastity filter, we demultiplexed the reads by index with no mismatches tolerated. We then merged overlapping reads using the approach outlined in Rokyta et al. (2012). This process removed adapter sequences and corrected sequencing errors in overlapping regions. After merging, we assembled the reads using the quasi-de-novo assembler outlined in Hamilton et al. (2016), with *Pseudacris nigrita* and *Gastrophyrne carolinensis* serving as divergent references. In order to avoid the potential effects of low-level contaminants, we removed assembly clusters containing fewer than 57 reads (the 5 %-tile of the read coverage distribution for the largest assembly cluster across loci). Finally, we constructed consensus sequences from the read assemblies, utilizing ambiguities when base frequency distributions at a site could not be explained by sequencing error (see Hamilton et al., 2016 for more details). In order to place the *Dendropsophus* samples within a broader context, we included 19 additional hylid samples from outside Dendropsophini, as well as one sample from Ceratophryidae. We obtained consensus sequences from these samples from previous studies (Barrow et al., 2018; Banker et al., 2020; Dolinay et al., 2021; Hime et al., 2021). Note that target loci from all of these studies corresponded to those of the Dendropsophini samples.

2.1.4. Orthology assessment and alignment generation

Following Hamilton et al. (2016), we assessed orthology by computing pairwise (alignment-free) distance matrices and clustering the homologous sequences using a neighbor-joining approach. After removing ortholog clusters containing less than 50 % of the samples prior to proceeding downstream, we aligned homologous sequences using Mafft (v7.023b, Katoh and Standley, 2013). To reduce the effects of missing data and misaligned sequences we applied the automated trimmer/masker described by Hamilton et al. (2016), with the MINGOODSITES parameter set to 14 and the PROPGOOD parameter set to 0.5. Sites represented by less than 50 % of the samples after masking were excised from the alignment. We visually inspected the resulting alignments in Geneious (R9, Biomatters Ltd., Kearse et al., 2012) to verify the alignments.

2.2. Sanger sequences and phenomic evidence

Sanger sequences and phenomic characters were derived from Orrico et al. (2021; hereafter called the SP data set). Among ingroup terminals, the AHE partition comprises a subset of the terminals analyzed by Orrico et al. (2021), with the addition of three undescribed species (*Dendropsophus* sp. sister species to *D. ozzyi, Dendropsophus* cf. *minutus,* and *Dendropsophus* sp. related to *D. shiwiarum*) and two of the four terminals identified as *D. brevifrons* (but see Discussion) represented only by AHE data (for information on outgroup sampling, see Table S1-S2). To accelerate analyses, we eliminated confirmed conspecific terminals (i.e., those whose uncorrected pairwise 16S distances were less than 3 %) but retained putatively conspecific terminals for which either molecular or morphological data suggested they might represent different species, and we did not delete any terminals for which AHE data were also obtained. To maximize the data coverage for included terminals, we merged missing Sanger fragments from excluded terminals with those of the included conspecific terminals.

Subsequent to the online release of Orrico et al. (2021) in June 2020, several publications related to *Dendropsophus* systematics were published (see Discussion). One of the candidate species identified by Orrico et al. (2021)—*D. decipiens* V—was described as *D. tapacurensis* by Oliveira et al. (2021), while *D. luddeckei* was placed in the synonymy of *D. molitor* by Árias-Cárdenas et al. (2024) and *D. koechlini* was placed in the synonymy of *D. pauiniensis* by Melo-Sampaio (2023). While we agree with these taxonomic changes, we have not incorporated these into our dataset. However, to facilitate comparison of the current results with those of Orrico et al. (2021), we did not include additional terminals or published data in our analyses. Specifically, we did not add *D. bilobatus* and the two candidate species associated with *D. reichlei* from Ferrão et al. (2020), *D. kubricki* from Rivadeneira et al. (2018), or *D. arndti, D. leucophyllatus, D. vraemi,* and candidate species D–G from Caminer et al. (2017). Likewise, we did not include the SNP data from Pirani et al. (2020); their results suggest that *D. ebraccatus* is composed of two independent lineages (one from Costa Rica and the other from Ecuador) but it is unclear which lineage(s) we have because our data are not directly comparable to Pirani et al. (2020) and indirect designation by geographic locality is not straightforward.

2.3. Phylogenetic analyses

2.3.1. Overview of analyses

To assess the impact of the new AHE data on our understanding of the *Dendropsophus* phylogeny, we analyzed the new AHE data set separately using (A) maximum likelihood (ML; AHE-only), (B) a coalescent species tree approach (AHE-only; ASTRID), and (C) maximum parsimony (MP; AHE-only). We also combined the AHE data with the Sanger sequences and phenomic characters (SP data set) of Orrico et al. (2021) and analyzed this total-evidence data set (AHE + SP) under (D) maximum likelihood and (E) maximum parsimony. Given that we employed a different method of alignment (similarity-alignment in MAFFT v7.023b, Katoh and Standley, 2013) than Orrico et al. (2021; tree-alignment in POY v.5.1.1; Wheeler et al., 2015) and treated gaps as missing nucleotides (gaps treated as insertion/deletion events by Orrico et al., 2021), we reanalyzed their data set of Sanger sequences and phenomic characters as well under ML (F) and MP (G). We selected outgroups based on current knowledge of hylid phylogenetic relationships (Araujo-Vieira et al., 2019; Araujo-Vieira et al., 2023; Hime et al., 2021; Orrico et al., 2021; Blotto et al., 2021). We included species of *Ceratophrys* (Ceratophryidae), *Litoria* (Pelodryadinae), *Xenohyla* (Hylinae, Dendropsophini), *Acris*, *Hyla*, and *Pseudacris* (Hylinae, Hylini), *Phyllodytes* and *Trachycephalus* (Hylinae, Lophyohylini), *Lysapsus* and *Scarthyla* (Pseudini), *Ololygon* and *Scinax* (Scinaxini), and *Gabohyla* and *Sphaenorhynchus* (Sphaenorhynchini). The trees were rooted with *Ceratophrys*.

2.3.2. Maximum likelihood analysis

We performed ML analyses using IQ-TREE multicore version iqtree-2.2.2.3 (Minh et al., 2020). We first used ModelFinder (Kalyaanamoorthy et al., 2017), spawned from IQ-TREE, to choose the best-fit substitution model and partition scheme for the AHE and Sanger data (option −m MF + merge). We used the two morphological models implemented in IQ-TREE (i.e., MK and ORDERED, for nonadditive and additive transformation series, respectively; for additivities see Orrico et al., 2021) with ascertainment bias correction. We obtained branch supports from 1000 ultrafast bootstrap replicates (Minh et al., 2013; Hoang et al., 2018).

2.3.3. Maximum parsimony analysis

We performed all MP analyses in TNT v1.5 (Goloboff et al., 2008; Goloboff and Catalano, 2016) using equal costs for all transformations, gaps treated as missing data, and stopping when a stable consensus was

reached five times (TNT command: xmult = level 10 chklevel 5 consense 5). We calculated jackknife frequencies from 1000 pseudoreplicates run in sets of 50 (TNR command: hold 5000; rseed 0; rseed*; resample jak savetrees freq replications 50 [xmult = replications 2 hits 2;]) and subsequently merged manually. We used the TNT script forfai.run written by Pablo A. Goloboff (available at https://www.lillo.org.ar/phylogeny/tnt/scripts/forfai.run), which takes as input the most parsimonious trees and the trees resulting from the resample pseudoreplicates and outputs a strict consensus with branch lengths and support values in Newick format. This file was read with FigTree v1.4.3 (Rambaut, 2009) for visualization and editing.

2.3.4. Tree comparisons

Using the packages ape v5.0 (Paradis and Schliep, 2019), phytools v2.1.1 (Revell, 2024), stringr (Wickham, 2023), and treedist v2.7.0 (Smith, 2020) in R v4.3.2 (R Core Team, 2023), we compared the strict consensus topologies and support values for shared and unshared clades of the SP-only and AHE + SP analyses and the AHE + SP and AHE-only analyses for both ML and MP analyses, as well as the ML and MP results for the SP, AHE-only, and AHE + SP characters analyses (i.e., F vs D, G vs E, A vs D, C vs E, etc). After parsing Newick or TNT trees containing support values and removing terminals that were not present in both trees, we proceeded to calculate the Robinson–Foulds distance (Robinson and Foulds, 1981) between each pair of trees and list all clades shared by both trees and all clades unique to each tree, together with their respective support values.

2.3.5. Coalescence: AHE-only

For the coalescent approach, we first estimated gene trees in RAxML (Stamatakis, 2006) under a GTRGAMMA model. To reconstruct the species trees from the gene trees obtained from the RAxML analysis, we estimated a genome-scale coalescent-based species tree using the program ASTRID (Vachaspati and Warnow, 2015). Because the maximum likelihood tree (A) and species tree (B) shared the same topology, we used only the species tree (B) for downstream ancestral state reconstruction.

2.4. Divergence-time estimation

We employed the results of analyses B and D (see Overview of Analyses above) for all downstream analyses. We employed a Bayesian molecular clock dating method that is appropriate for genome-wide datasets, MCMCTree from PAML v4.9j (dos Reis and Yang, 2019). MCMCTree uses fossil constraints to estimate divergence times within a phylogeny under multiple molecular clock models. We used four fossil-informed node dates for the calibration (Table 1).

We utilized a uniform prior for the most recent common ancestor (MRCA) of Hylidae and its sister group of between 125 mya (Báez et al., 2009) and 33.9 mya (*Hyla swanstoni* fossil; Holman, 2003, Holman, 1968; Table 1). We follow Wiens et al.'s (2006) interpretation of the MRCA of the *Acris–Pseudacris* clade, utilizing a fossil identified as the extinct taxon *Acris barbouri* (likely the sister group to an extant *Acris* species) dated at least 15–19 mya (Holman, 2003; Table 1). In addition, we define the MRCA of the *Hyla squirella–Hyla cinerea* clade as at least 15 mya based in the fossil species *Hyla goini* (thought to be closely related to, if not conspecific with, extant *H. squirella*; Sanchiz, 1998) dated at 15–19 mya (Holman, 2003; Table 1). Finally, we define the MRCA of the *Hyla gratiosa–Hyla versicolor* clade as at least 16 mya based on two fossils: *Hyla miocenica* (thought to be closely related to *Hyla chrysocelis* and *H. versicolor*) dated at 14–16 mya and the fossil of *Hyla miofloridana* (a species similar to *H. gratiosa*) dated at 15–19 mya (Holman, 2003; Table 1).

Table 1
Fossil calibrations employed for the divergence-time estimate of *Dendropsophus*.

Taxonomic group	Fossil Date	Source
Hylidae and sister group	125 – 33.9 mya	Lower bound- *Hyla swantsoni* (Holman 2003; Holman 1968); Upper bound- older remains of *Eurycephala alcinae* and *Araryphrynus placidoi* Báez et al. (2009)
Acris + *Pseudacris*	>15 mya	Holman (2003)
Hyla squirella + *Hyla cinerea*	>15 mya	Holman (2003)
Hyla gratiosa + *Hyla versicolor*	>16 mya	Holman (2003)

A caveat regarding these calibrations is that no synapomorphic evidence associates any of these fossils with the clades to which they have been referred, with some of these relationships being openly questioned (e.g., *Hyla swanstoni*; Sanchiz, 1998). All of the abovementioned fossil taxa are known exclusively from ilia or, in the case of *Hyla swanstoni*, ilia and partial tibiofibulae, and no synapomorphy involving ilial or tibiofibular morphology has so far been proposed for hylids. Further, all of the associations were made prior to the major overhaul of hylid relationships of the mid-2000 s (e.g., Faivovich et al., 2005) within a very different phylogenetic context from what we now know, meaning that, in the case of *Hyla* and *Acris–Pseudacris*, these fossils apparently were never compared with most of the intervening taxa between these two distant clades of Hylini or any of the other hyline tribes.

We added the four fossil calibrations to the respective nodes of the tree with lower bound priors, default *p* values of 0.1, and *c* values of 0.2. The gradient and Hessian matrices were calculated with the *usedata = 3* option. One partition was used for all loci with independent rates molecular clock model and a GTR + Γ model of nucleotide substitution. An alpha value of 0.35 was used, as 0.35 was the average alpha from the RAxML analysis. The alpha parameter is the shape parameter of the mutation rate. A low alpha value (<1) suggests that the distribution of mutations across the alignment is tightly clustered and approximates a negative binomial distribution, indicating that some sites do not mutate at all and a small number of sites mutate a lot. An estimated mean substitution rate for the amphibian clade of 0.899 substitutions per million years from Hime et al. (2020) was used to parameterize a diffuse gamma Dirichlet prior Γ(a b) on locus rates (*rgene_gamma*) as Γ(1 111), where a = 1 and b = 111. This sets a gamma prior for the mean rate across loci, and a Dirichlet distribution is used to partition the prior across loci. The gamma distribution has mean a = b and variance a = b^2. The first parameter (a) controls the shape of the distribution. Values of a = 1 or = 2 lead to fairly diffuse priors. We set this value to 1, and then fixed b so that the mean rate matched the estimated mean substitution rate proposed by Hime et al., 2020. We ran MCMC chains for 1,000,000 total generations, with 1,000,000 burnin generations, and 100 generation sampling frequency. Additionally, we utilized the function ltt (Pybus and Harvey, 2000) from the phytools package (Revell, 2012) in R to create a lineage through time plot for calculating Pybus and Harvey's "gamma" statistic to determine if *Dendropsophus* diversified with constant rates.

2.5. Biogeographic analyses

2.5.1. Ancestral range estimation

To estimate the ancestral geographic range of *Dendropsophus*, we employed a maximum likelihood approach to ancestral range estimation using the R program BioGeoBEARS (Matzke, 2013). This analysis provided geographic range estimates for each node of the *Dendropsophus* phylogenetic tree estimated from the previous analysis. We utilized the Dispersal–Extinction–Cladogenesis (DEC) model as it allows for the estimation of range transitions as a function of time (Ree and Smith, 2008), enabling us to use the dated *Dendropsophus* phylogenies B and D, to test specific hypotheses of evolutionary biogeography. Each *Dendropsophus* species was assigned a "state" corresponding to its geographic range. This consisted of a specific combination of presences and absences in the biomes of Central and South America (Fig. 1). We

defined a total of seven geographic areas (Fig. 1; Batalha-Filho et al., 2013; Ledo and Colli, 2017). Geographic areas were defined as seen in Fig. 1 to balance increased specificity and computational effort; this assignment maximized the number of geographical areas (greatest specifications) before computational constraints became too high for the program to handle. We ran 50 DEC models and recorded the number and type of events from each model. We calculated and compared ML state probabilities and averages from Biogeographic Stochastic Mapping (BSM) values from the DEC models. All additional parameters of the model were set as the default standards; for a full description and explanation of each default standard, see Dupin et al (2016) and Matzke (2016).

2.6. Oviposition site evolutionary analyses

2.6.1. State dependent diversification models

We scored species oviposition site as either aquatic or terrestrial egg deposition based on available direct observation data for 47 % of the 78 species in the genus (Crump, 1974; Duellman, 1978; Weygoldt and Peixoto, 1987, Mageski et al., 2014; Orrico et al., 2021; Schiesari et al., 2022). We utilized a Markov chain Monte Carlo Bayesian approach to estimate ancestral character states of phylogenies B and D through the program RevBayes (Höhna et al., 2014; Höhna et al., 2016). To estimate the ancestral oviposition sites of *Dendropsophus*, we employed a multi-state MCMC model (at least 10,000 total generations, 2,000 burnin generations, 100 sampling frequency). To determine whether oviposition site has an impact on lineage accumulation rate in the clade we employed both a Binary state speciation and extinction model (BiSSE) and a Hidden state speciation and extinction model (HiSSE) using RevBayes (Höhna et al., 2014, 2016). We ran an MCMC of at least 10,000 total generations, 2,000 burnin generations, and 100 sampling frequency for each model.

2.6.2. Comparative analysis

To test for a correlation between the transition to a terrestrial oviposition site and a species' geographic expansion to more than one geographic range we employed a correlated evolution model via RevBayes (Höhna et al., 2014; Höhna et al., 2016). The binary character matrix for egg deposition site from the analysis above was utilized (where 0 = aquatic egg deposition and 1 = terrestrial egg deposition). We created a binary state character for species' geographic range, where species ranges were coded as 0 = one geographic range or 1 = more than one geographic range. We ran an MCMC of 10,000 total generations, 200 burnin generations, and 200 sampling frequency for each model.

3. Results

3.1. Anchored hybrid enrichment data

Our AHE analyses recovered 432 orthologous nuclear loci for the 78 *Dendropsophus* and 20 outgroup taxa. This number of loci was greater than the number targeted by our hybrid enrichment kit because the target probes bind to sequences up to 30 % divergent including deeply diverged gene duplicates. Sixty-eight duplicates were identified and separated as additional informative loci for this study. The average locus length across all loci was 1562 base pairs. Of the 655,061 aligned sites, 287,758 were variable and 228,603 were parsimony informative. The quantity of missing data was low (8.59 % missing characters).

3.2. Phylogenetic relationships

The results of all the phylogenetic analyses (A–G) are provided in the main text or as supplementary files (Fig. 2a [analysis E]; Figs. S1-S6 [analyses A-D, F-G]). The monophyly of Dendropsophini (*Xenohyla* + *Dendropsophus*) was supported in all analyses, as was the monophyly of most of the species groups, clades, and complexes named by Orrico et al. (2021; Figs. 2b and c; Table 2). All analyses also agreed in refuting the monophyly of the *D. leucophyllatus* group, and within it the proposed *D. haraldschultzi* and *D. leucophyllatus* clades, as well as the *D. nanus* clade (within the *D. microcephalus* group). Disagreements among analyses include the *D. ruschii* group, which was only monophyletic in the strict consensus from analysis G (Fig. S9), the *D. marmoratus* group, which was rejected in the tree from analysis F, the *D. parviceps* group, which was nonmonophyletic in the tree from analysis F (Fig. S8), and the *D. antaliasiasi* complex (within the *D. microcephalus* group, *D. rubicundulus* clade), which was rejected in phylogenies from analyses A and D (Figs. S1 and S4, respectively). Below we summarize numerical comparisons of the analyses (see also Table 3).

3.2.1. Maximum likelihood comparisons

Adding AHE data to SP data in the combined analysis increased the average bootstrap value over the analysis of SP data alone (trees from analyses D vs. F, respectively; Table 3). Phylogenies from D and F shared 174 clades (83 %). Support values were identical for 155 (89 %) of those clades, but inclusion of the AHE data increased support by 1–38 % for 11 clades (6 %) and decreased support by 1–40 % for 8 clades (5 %). Among the 35 clades in analysis F tree that were refuted by inclusion of the AHE data, support was > 90 % for 25 clades (100 for 16 clades) and < 70 % for only two clades. Similarly, among the 35 clades that are unique to the tree from analysis D, support was > 90 % for 20 clades (100 for 16 clades) and < 70 % for three clades. In the tree from analysis F, the *D. marmoratus* and *D. parviceps* groups are nonmonophyletic, with the species of the *D. marmoratus* group having a deeper coalescence than those of the *D. parviceps* group. In contrast, in the tree from analysis D, both groups are monophyletic, with the *D. parviceps* group originating earlier than the *D. marmoratus* group.

Excluding SP data from the combined analysis and analyzing AHE data alone increased the average bootstrap score (trees from analyses D vs. A, respectively; Table 3). Phylogenies from D and A were almost identical, sharing 122 clades (99 %) and differing in only a single clade each (1 %) involving the placement of *D. cachimbo* 2 and *D. rozenmani* 1; both clades were poorly supported (< 70 %; Table 2). Inclusion of the SP data increased support for four clades (3 %) and decreased support for 15 clades (12 %), with the remaining 103 (84 %) unchanged.

3.2.2. Maximum parsimony comparisons

Including AHE data with SP data in a combined analysis increased the average bootstrap value over the analysis of SP data alone (strict consensus of analyses E vs. G; Table 3). For the 165 clades shared by the strict consensus from analyses E and G, inclusion of the AHE data increased support by 1–41 % for 37 (22 %), decreased support by 1–19 % for 17 (10 %) and had no effect for the remaining 111 (68 %). Among the 35 clades in the tree from analysis F that were refuted by inclusion of the AHE data, support in the tree from analysis D was > 90 % for 25 clades (100 for 16 clades) and < 70 % for only two clades. Similarly, among the 35 clades that are unique to the tree from analysis D, support in the tree from analysis F was > 90 % for 20 clades (100 for 16 clades) and < 70 % for three clades. The most immediately obvious difference between the trees from analyses E and G is that inclusion of the AHE data resolves the polytomies among the species groups. Specifically, the strict consensus from analysis G includes a trichotomy between the clade composed of the *D. columbianus* + *D. molitor* groups, the *D. parviceps* group, and another polytomy composed of the species of the non-monophyletic *D. leucophyllatus* group and the *D. marmoratus*, *D. minutus*, and *D. microcephalus* groups. In contrast, both polytomies are resolved in tree E.

Excluding SP data from the combined analysis and analyzing AHE data alone increased the average bootstrap score (tree E vs. C, respectively; Table 3). As in the ML analyses, the trees from analyses C and E were almost identical, sharing 118 clades and differing in only three clades present in the tree from C but absent from the consensus tree from E (no clades present in E were absent from C). In the first of these clades,

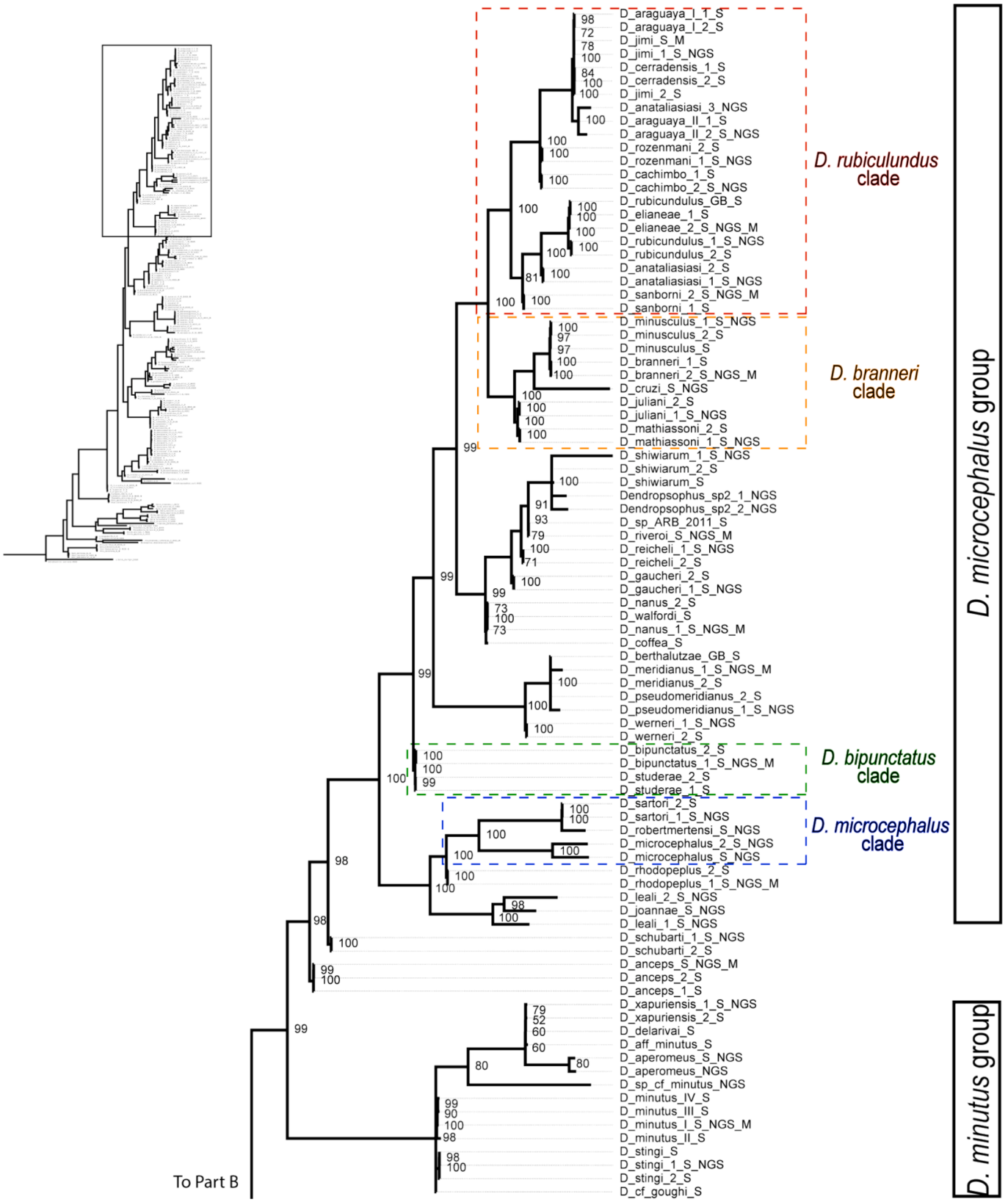

Fig. 2a. Maximum parsimony tree (E) estimated using TNT from combined AHE + SP data. Jackknife values are presented at each node. Note the two *D. schubarti* and three *D. anceps* terminals are unassigned to a *Dendropsophus* group. Taxon names correspond to Table S1.

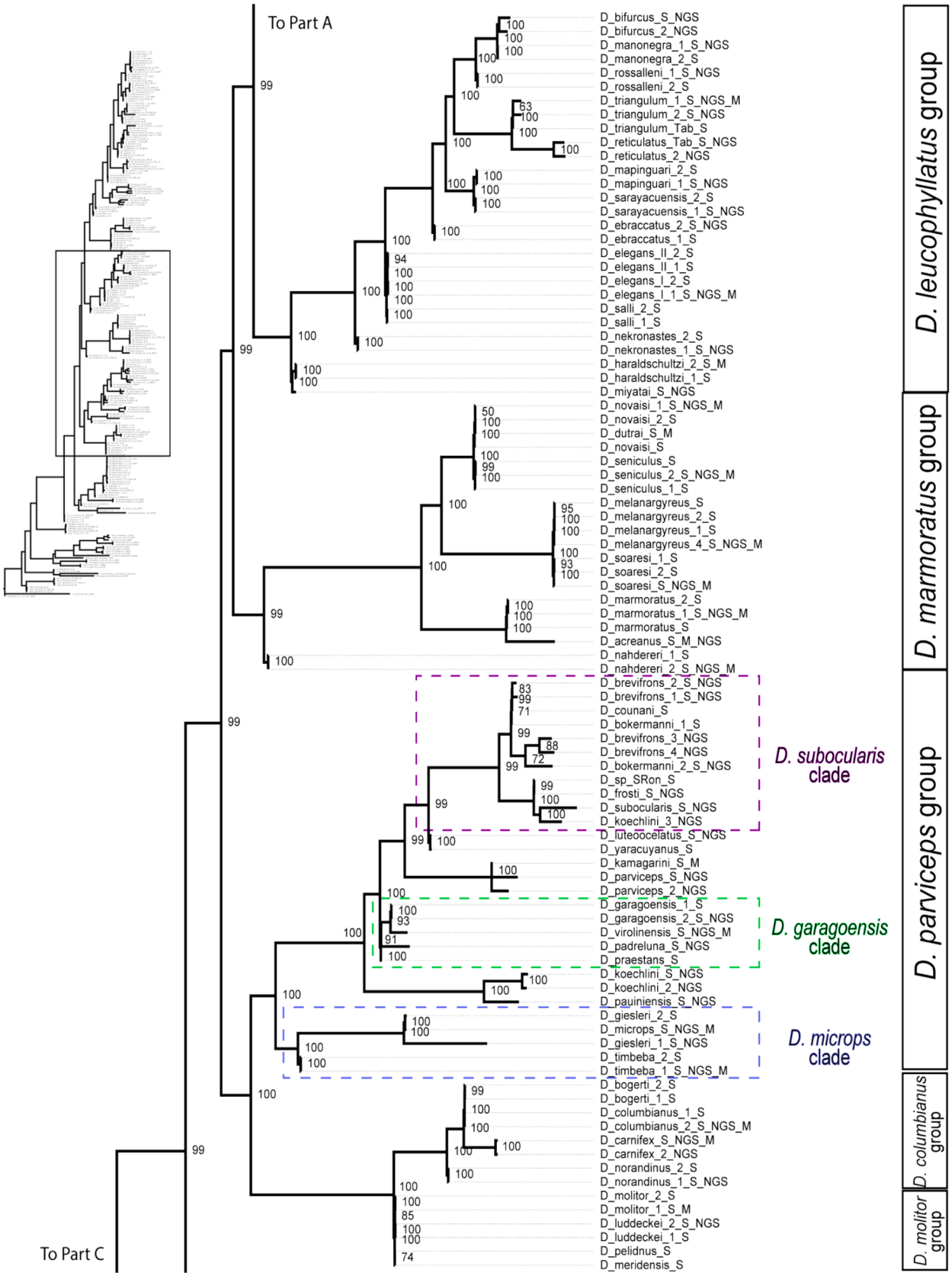

Fig. 2b. Maximum parsimony tree (E) estimated using TNT from combined AHE + SP data. Jackknife values are presented at each node. Taxon names correspond to Table S1.

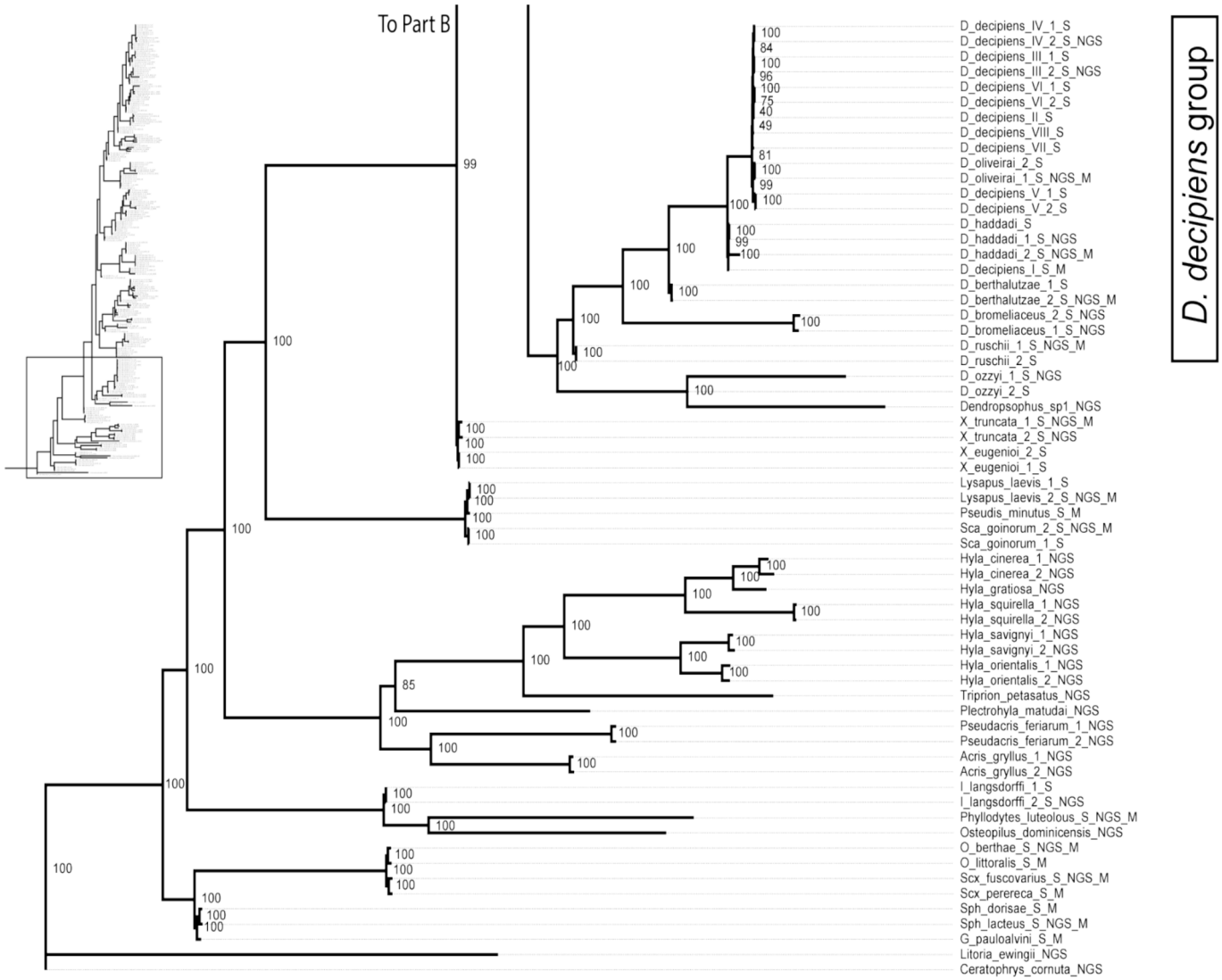

Fig. 2c. Maximum parsimony tree (E) estimated using TNT from combined AHE + SP data. Jackknife values are presented at each node. Note the two *D. ozzyi* and the *D. sp 1* terminals are unassigned to a *Dendropsophus* species group. Taxon names correspond to Table S1.

D. cachimbo 2 is the sister lineage to *D. jimi* 1 + *D. aragauaya* II (support = 49 %) in the tree of analysis C, whereas *D. cachimbo* 2 and *D. jimi* 1 + *D. aragauaya* II form a trichotomy with *D. rozenmani* 1 in the strict consensus of analysis E. The second clade that is absent from the strict consensus of analysis E is *Dendropsophus* sp2 1 + *Dendropsophus* sp2 2 (support = 100 %), which is the sister group to *D. shiwiarum* 1 in the tree of analysis C but collapses into a trichotomy with *D. shiwiarum* 1 in the strict consensus of analysis E. The third clade is *D. minutus* I + *D. stingi* 1 (support = 100 %), which form a trichotomy with the clade composed of *D.* sp. cf. *minutus*, *D. xapuriensis*, and the two specimens of *D. aperomeus* in the strict consensus of analysis E. Among the 118 shared clades, inclusion of the SP-only dataset increased support by 1–23 % for two clades (2 %) and decreased support by 1–40 % for 36 clades (30 %), with the remaining 80 clades (68 %) unchanged.

3.2.3. ML–MP comparisons

ML produced higher average bootstrap values than MP for all comparisons (Table 3). Among the 178 clades shared by the ML and MP trees for the SP-only dataset (F and G, respectively), support was identical in 120 clades (67 %). The support values of 58 clades (33 %) differed between trees F and G, being higher for F in 57 (32 %) and higher for G in only 1 (0.6 %). The strict consensus from analysis G includes 18 clades that were absent from analysis F, among which support in G was > 90 % for two clades (100 % for one clade) and < 70 % for 10 clades. The tree from analysis F lacks polytomies and therefore includes 31 clades that are absent in the strict consensus from analysis G; support in F was > 90 % for 19 clades (100 % for six clades) and < 70 % for only three clades.

The ML and MP trees for the AHE-only dataset (analyses A and C, respectively) were much more similar (RF = 5), sharing 118 clades and differing in only three clades present in C but absent in A (support in C = 58 %, 100 %, and 100 %) and two clades present in A and absent in C (support in A = 72 % and 78 %). Among the 118 shared clades, support was identical for 112 clades (95 %), almost all of which were 100 %. For the remaining four clades, support was higher in C for two clades and higher in tree A for two clades.

Fifty-four (25 %) of the 213 clades shared by the ML and MP trees from the AHE + SP analyses (D and E, respectively) differ in support, with five (2 %) being higher in E and the remaining 49 (23 %) being higher in D. Support was 100 % for all 159 (75 %) of the clades with the same support in both analyses. The MP tree includes 16 clades unique to it, four of which had support > 90 % (100 % for two clades) and six had support < 70 %. Due to the lack of polytomies, the tree from analysis D includes 28 clades unique to it, almost twice as many as the strict consensus tree from analysis E, among which support is > 90 % for 14

Table 2
Dendropsophus species groups, clades, and complexes recognized by Orrico et al. (2021) and their monophyly (+) and non-monophyly (–) resulting from maximum likelihood (ML) and maximum parsimony (MP) analyses of the anchored hybrid enrichment (AHE), Sanger + phenomic characters (SP) and their combinations (see Overview). Analyses that did not include more than one species to test the monophyly of a given group are indicated as NA. Letters in top row correspond to the phylogenetic analyses outlined in the Overview (see Methods).

	(D) ML AHE + SP	(E) MP AHE + SP	(F) ML SP-only	(G) MP SP-only	(A) ML AHE-only	(C) MP AHE-only
D. ruschii group	–	–	–	+	–	–
D. decipiens group	+	+	+	+	+	+
D. parviceps group	+	+	–	+	+	+
D. subocularis clade	+	+	+	+	+	+
D. microps clade	+	+	+	+	+	+
D. garagoensis clade	+	+	+	+	+	+
D. molitor group	+	+	+	+	NA	NA
D. columbianus group	+	+	+	+	+	+
D. marmoratus group	+	+	–	+	+	+
D. minutus group	+	+	+	+	+	+
D. leucophyllatus group	–	–	–	–	–	–
D. *haraldschultzi* clade	–	–	–	–	–	–
D. leucophyllatus clade	–	–	–	–	–	–
D. microcephalus group	+	+	+	+	+	+
D. microcephalus clade	+	+	+	+	+	+
D. bipunctatus clade	+	+	+	+	+	+
D. nanus clade	–	–	–	–	–	–
D. branneri clade	+	+	+	+	+	+
D. rubicundulus clade	+	+	+	+	+	+
D. anataliasiasi complex	–	+	+	+	–	+
D. araguaya complex	+	+	+	+	+	+

clades and < 70 % for 10 clades.

3.3. Divergence-time estimation

The divergence time for the origin of *Dendropsophus* was estimated at approximately 57.05 mya (66.95–46.71 mya, 95 % CI; Fig. 3) on the ASTRID tree (B). The estimated *Dendropsophus* divergence time on the ML total-evidence tree (D) was 57.43 mya (67.21–47.37 mya, 95 % CI; Fig. S7). This divergence falls before the timing of the Andean uplift 40–24 mya in the Miocene (Batalha-Filho et al., 2013; Fig. 1). The dynamic nature of the junction between Amazonia and the Atlantic Forest during this time, and the estimate of *Dendropsophus* divergences within this period, provide multiple opportunities for geographic expansion and fragmentation of population lineages which we explore further below. The lineage accumulation through time within the clade is visualized in Fig. 4. Our analyses estimated Pybus and Harvey's "gamma" statistic at gamma = 0.9603, p-value = 0.3369, suggesting that *Dendropsophus* experienced episodes of expansion and fragmentation throughout its history from Miocene to present.

3.4. Biogeographic history

All dispersals estimated for *Dendropsophus* under the three dispersal hypotheses are range-expansion dispersal events, and none of the models were consistent with extinction or range-switching. The MRCA of five of the nine species groups of *Dendropsophus* (as defined in Orrico et al., 2021) were estimated to fall within the uplift of the Andes (Fig. 3; ML tree Fig. S7). The MRCA of *Dendropsophus* is inferred to have spanned the Atlantic Forest and Amazonian-Orinocan Lowland and to have expanded multiple times into the surrounding Central and South American biomes (Fig. 5; ML tree Fig. S8). Specific dispersal events estimated by the BioGeoBEARS analysis (Table S3; ML tree Table S6) during the Andean uplift can be seen in the most likely ancestral range estimation (Fig. 5; ML tree Fig. S8). The combination of these outputs shows a vicariance event that appears to have split *D. ozzyi* from the members of the *D. decipiens* group, where *D. ozzyi* dispersed to the Amazonian-Orinocan Lowland and the *D. decipiens* group dispersed to the Atlantic Forest (Fig. 5). The *D. molitor* group separated from the *D. parviceps* group through a vicariant event to the Andes while the *D. parviceps* group expanded their range from the Atlantic Forest into Amazonia (Fig. 5). The *D. minutus* group originated via a range expansion from Amazonia to the Andes and Atlantic Forest, and the *D. leucophyllatus* group via a range expansion to Amazonia (Fig. 5). Finally, the *D. microcephalus* and *D. marmoratus* groups originated in the Atlantic Forest but further speciated following multiple range expansions (Fig. 5). These results suggest that most species groups of *Dendropsophus* originated via range expansion speciation events followed by geographic fragmentation.

3.5. Oviposition site state dependent diversification and comparative analyses

At least three independent transitions from aquatic to terrestrial oviposition site have occurred in *Dendropsophus* (Fig. 6; ML tree Fig. S9). Aquatic egg deposition was estimated as the ancestral state for *Dendropsophus* (aquatic egg deposition state likelihood = 90.91 %; Fig. 6). There was no correlation between lineage accumulation rate and egg deposition site. The lineage accumulation rate for species with an aquatic egg deposition site was estimated to be 0.8196 (sd = 0.2146) changes per time unit and 1.9916 (sd = 0.4445) changes per time unit for species with a terrestrial egg deposition site (Table S5, Fig. 7; ML tree Table S8, Fig. S10). The HiSSE revealed a clear hidden state underlying variance in diversification-rate differences within clades of each egg deposition site (Fig. 6; ML tree Fig. S9). Furthermore, we did not find a correlation between the probability of gaining or losing terrestrial or aquatic egg deposition and inhabiting more than one geographic range (Fig. 6; ML tree Fig. S10).

4. Discussion

4.1. Phylogenetic relationships of Dendropsophus

The current study employed more than 100 times more data to test the phylogenetic relationships among species of *Dendropsophus* than were analyzed previously (Orrico et al., 2021). Given the magnitude of this empirical contribution, a major objective of the present study was to evaluate the extent to which previous results withstood or were overturned by such a massive expansion in data. It is evident that some of the deviations of our results from those of Orrico et al. (2021) are due to the method of alignment and/or treatment of gaps—tree-alignment and gaps treated as insertion/deletion events in Orrico et al. (2021), similarity-alignment and gaps treated as missing nucleotides here—and not the addition of the AHE data. For example, Orrico et al. (2021) found the *D. leucophyllatus* group and the proposed *D. haraldschultzi*, *D. leucophyllatus*, and *D. nanus* clades to be monophyletic, but all of our analyses rejected them, including our reanalysis of the SP-only dataset from Orrico et al. (2021). This finding that the method of alignment and treatment of gaps can have important effects on relationships and support is consistent with previous reports that those analytical parameters can be more significant than choice of optimality criterion or

Table 3
Summary of the comparisons between the strict consensus trees obtained from maximum likelihood (ML) and maximum parsimony (MP) analyses of the AHE, SP, and AHE + SP datasets (A, C–G), including the Robinson–Foulds distance (RF), number of shared clades, number of unique clades, and the corresponding support values. Support is summarized as the mean (minimum–maximum). The tree column indicates the phylogenies estimated from analyses outlined in the Overview (see Methods). The Robinson–Foulds distance is a measure of dissimilarity between two phylogenetic trees; this metric is calculated by counting the number of unique clades present in one tree and not the another. Overall, analyses including AHE data produced higher average bootstrap values. Adding SP data to AHE-only analyses decreased average branch support. ML generated higher average support values than MP analyses.

Comparison	Analysis	RF	# shared clades	Support shared clades Tree 1	Support shared clades Tree 2	# unique clades Tree 1	Support unique clades Tree 1	# unique clades Tree 2	Support unique clades Tree 2
Tree 1: ML AHE + SP **Tree 2:** ML SP	DF	70	174	98.8 (53–100)	98.6 (61–100)	35	90.2 (50–100)	35	92.7 (48–100)
Tree 1: ML AHE + SP **Tree 2:** ML AHE-only	DA	2	122	96.7 (45–100)	99.4 (72–100)	1	60	1	54
Tree 1: MP AHE + SP **Tree 2:** MP SP	EG	66	165	96.6 (49–100)	94.3 (31–100)	36	93.8 (40–100)	31	79.3 (42–100)
Tree 1: MP AHE + SP **Tree 2:** MP AHE-only	EC	3	118	97.1 (60–100)	99.4 (58–100)	0	NA	3	49–100
Tree 1: MP SP **Tree 2:** ML SP	GF	48	178	94.4 (44–100)	99.2 (69–100)	18	68.0 (31–100)	31	88.7 (48–100)
Tree 1: MP AHE-only **Tree 2:** ML AHE-only	CA	3	118	99.3 (49–100)	99.4 (54–100)	3	86.0 (58–100)	2	75.0 (72–78)
Tree 1: MP AHE + SP **Tree 2:** ML AHE + SP	ED	43	213	97.8 (50–100)	99.3 (60–100)	16	74.1 (40–100)	28	81.6 (45–100)

substitution model (Padial et al., 2014).

Although including AHE data increased average branch support in all comparisons, quantitatively the overall effect of the AHE data on both the topology and support values was modest. Under both ML and MP, more than 80 % of the clades supported in the AHE + SP analyses were also supported in the SP-only analyses (Table 3). Three taxonomically relevant differences, however, are attributable to the inclusion of the AHE data (viz., the non-monophyly of the *D. ruschii* group in the MP analysis and the *D. marmoratus* and *D. parviceps* groups in the ML analysis). Similarly, support was unchanged for most shared clades (89 and 68 % under ML and MP, respectively), and among those that differed, approximately the same number of clades increased as decreased under ML, and approximately twice as many clades increased as decreased under MP.

Nevertheless, although the changes caused by the inclusion of the AHE data were few in terms of taxonomic differences and the number of clades that were refuted or had increased/decreased support, this strictly quantitative perspective does not fully capture the contribution of the AHE data. Most importantly, the AHE data provided crucial evidence throughout the tree. This effect of AHE data is most clear in the MP analyses, in which the inclusion of the AHE data resolved the polytomies among the species groups, but it is also apparent in the monophyly and position of species groups in the ML analyses. Similarly, the AHE data also affected many relationships within groups under both optimality criteria (e.g., relationships among *D. decipiens* lineages). Indeed, the nearly identical topologies and support values for the AHE + SP and AHE-only analyses under both optimality criteria underscore the relevance of the AHE data.

Support values were an unreliable predictor of whether or not a given clade would be corroborated or refuted when the AHE data were added to the SP dataset. Clades with support as low as 61 (ML) and 31 (MP) in the SP-only analyses were corroborated when the AHE data were included. Similarly, among the clades that were refuted when the AHE data were included, support was 100 for 33 %, > 90 for 56 %, and < 70 for only 13 %. We caution that we calculated support using bootstrap (ML) and jackknife (MP) frequencies, and other measures of support (e.g., difference in log-likelihoods, *S*, or Goodman-Bremer support; (Edwards, 1972; Goodman et al., 1982; Bremer, 1988)) could behave differently (e.g, Machado et al., 2022).

Choice of optimality criterion minimally affected the results of the AHE + SP analyses, although ML produced higher branch support on average than MP. ML and MP consensus trees were highly congruent, with 91 % of the MP clades present in the ML tree and 85 % of the ML clades present in the MP tree, the main difference owing to the absence of polytomies in the ML tree. Support values more reliably predicted which clades would be absent in the other tree for MP than for ML. For MP, support was > 90 for 11 % of the unique clades and < 70 for 56 % of the unique clades. In contrast, for ML support was > 90 for 61 % of the unique clades and < 70 for only 10 %.

To avoid the paraphyly of the *Dendropsophus ruschii* group with respect to the *D. decipiens* group, we transfer *D. ruschii* to the *D. decipiens* group (thereby extinguishing the *D. ruschii* group). *Dendropsophus ozzyi*, a species for which only adult external morphology and vocalizations are known (Orrico et al., 2021), and one undescribed species are unassigned to any species group until data on larvae and reproductive biology become available.

The monophyly of the *Dendropsophus leucophyllatus* group as proposed by Orrico et al. (2021) is not supported by our results due to the relationships of *D. anceps* and *D. schubarti*. In their results, the group included two major clades, one that included *D. anceps* as the sister taxon of a clade that includes all other species traditionally assigned to the *D. leucophyllatus* group (the *D. leucophyllatus* clade), and another clade composed of *D. haraldschultzi*, *D. miyatai*, and *D. schubarti* (the *D. haraldschultzi* clade). In our results, *D. anceps* and *D. schubarti* are recovered as successive sister taxa of the *D. microcephalus* group as defined by Orrico et al. (2021). Both *D. anceps* and *D. shubarti* have a convoluted history of systematic arrangements. Nevertheless, this is the first time that both are recovered as closely related with the *D. microcephalus* group; one of the most characteristic groups of *Dendropsophus*, with nine phenomic synapomorphies inferred by Orrico

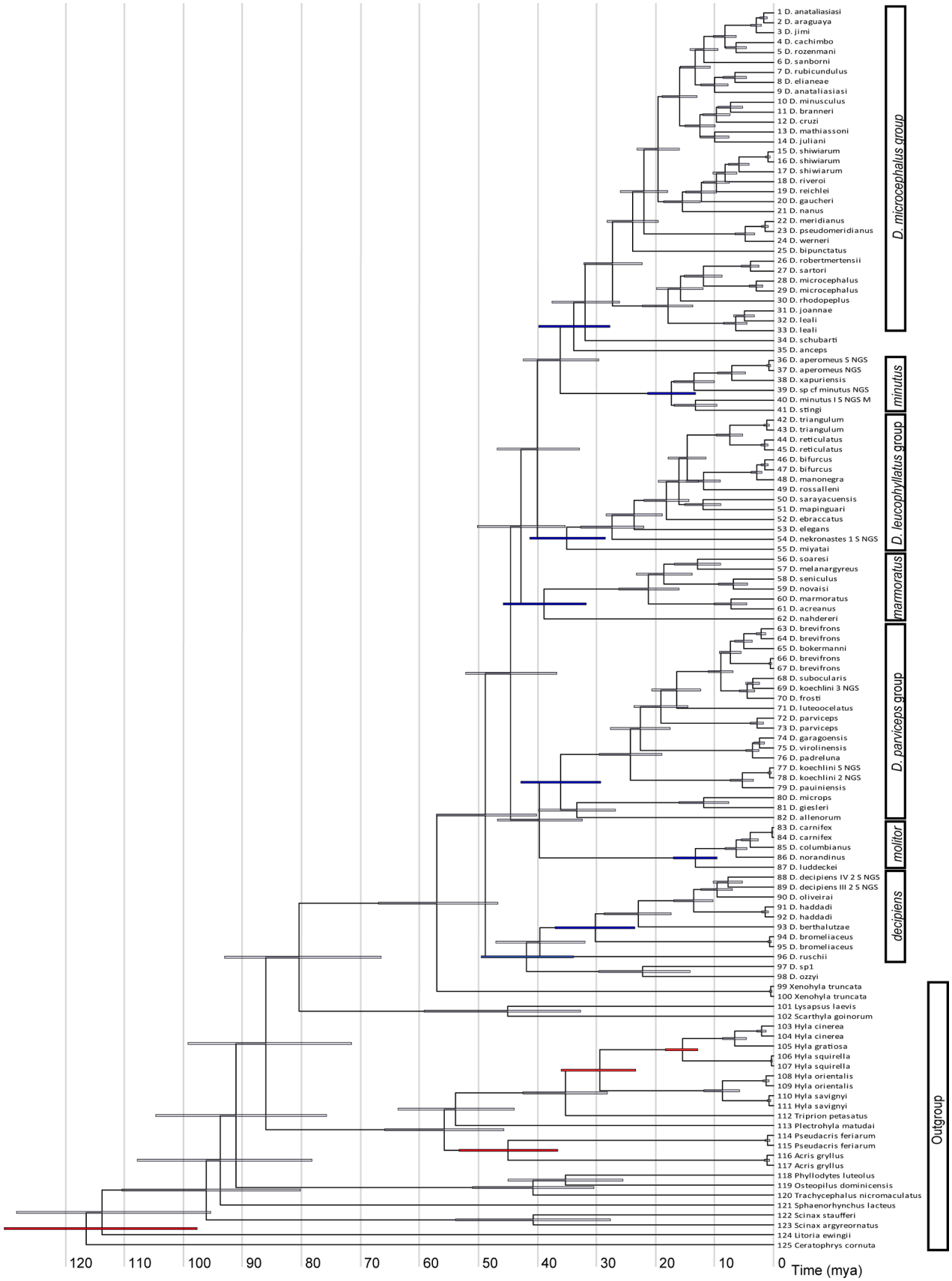

Fig. 3. Divergence time estimation of *Dendropsophus* and outgroups with 95% CI bars (red, fossil nodes and blue, *Dendropsophus* clades) for the dating estimate of each node on the ASTRID tree (B). Branch lengths are proportional to time. Taxon names correspond to Table S2. (For interpretation of the references to colour in this figure legend, the reader is referred to the web version of this article.)

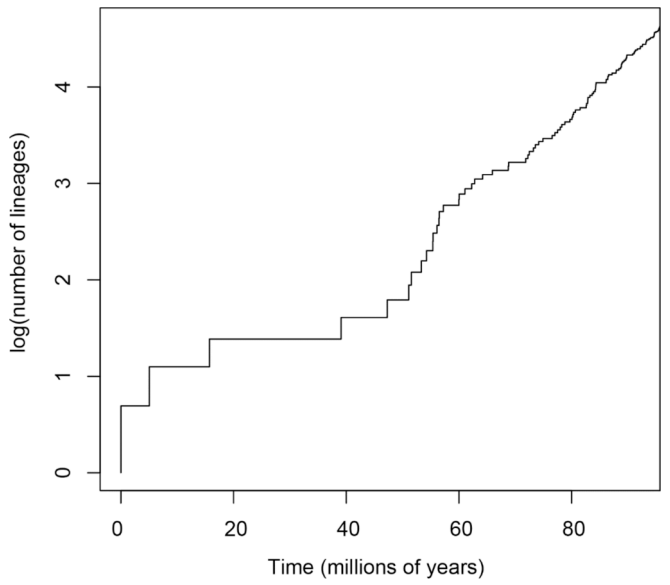

Fig. 4. Lineage through time plot of *Dendropsophus* and outgroups on the ASTRID tree (B). Number of lineages on the y axis is on a logarithmic scale. Lineage accumulation is the formation of lineages that leave descendants living today. Lineage accumulation/diversification does not deviate from constant within the clade (Pybus and Harvey's gamma = 0.9603, p-value = 0.3369).

et al. (2021).

Dendropsophus schubarti is a poorly known species, and its tadpole and calls are unknown. It has been suggested to be related to the groups of *D. leucophyllatus* (e.g., Bokermann, 1963; Orrico et al., 2021), *D. parviceps* (e.g., Bokermann, 1964; Duellman, 2001), or *D. marmoratus* (e.g., Fouquet et al., 2011). It has one or two suborbital bars, a light brown dorsum, and yellow flash colors on the thighs; all these character states are either homoplastic with distantly related species or plesiomorphic at this level. *Dendropsophus anceps* is unique in terms of both adult and larval external morphology (Lutz, 1973; Wogel et al., 2000) and has been recovered, usually with weak support, with the *D. leucophyllatus* group (Faivovich et al., 2005; Rivera-Correa and Orrico, 2013; Orrico et al., 2021), but not always (Jungfer et al., 2010; Peloso et al., 2016; Pirani et al., 2020). Phenotypically, it shares the bright red flash colors and two-note advertisement call with with the *D. leucophyllatus* group, two character states that show some homoplasy in *Dendropsophus*. Rivera-Correa and Orrico (2013) also suggested that the male pectoral glands are a putative synapomorphy, but Orrico et al. (2021) and our observations corroborate that males lack pectoral glands (while the females have them). We exclude *D. anceps* and *D. shubarti* from the *D. leucophyllatus* group to avoid its polyphyly, and for the time being, we leave these two species unassigned to any species group, pending the availability of phenomic data for *D. shubarti*. The presence of pectoral glands in males (c. 161) is a phenomic synapomorphy for the *D. leucophyllatus* group as redefined here.

Other topological differences between our results and those of Orrico et al. (2021) relate to alpha-taxonomic issues. These are the paraphyly of *Dendropsophus leali* with respect to *D. joannae* and the paraphyly of *D. nanus* with respect to *D. walfordi*. *Dendropsophus leali* and *D. joannae* are rather similar species both in external morphology and advertisement calls (Köhler and Lötters, 2001), and their taxonomic status requires further investigation. Seger et al. (2021) suggested the existence of up to four cryptic species in respect to calls and morphology in order to avoid considering *D. walfordi* junior synonym of *D. nanus*. The non-monophyly of samples identified as *D. brevifrons* and *D. bokermanni* suggest that our samples could correspond to additional, different species.

4.2. Evolutionary origin, divergence, and dispersal of Dendropsophus

We found an estimated divergence of *Dendropsophus* from other hylids at ~ 57 mya, somewhat older than previous estimates based on broader taxonomic sampling—previous estimates range from ~ 30 mya (Hedges et al., 2015; Portik et al., 2023) to 49.6 mya (Pyron, 2014). Our older divergence time for *Dendropsophus* likely differs due to our expanded prior for the date of the most recent common ancestor for Hylidae and its sister group and our more constrained taxonomic sampling. We placed the upper bound of this prior at 125 mya based on the fossil remains of *Eurycephalella alcinae* and *Arariphrynus placidoi* (Báez et al., 2009). Other studies (for example Wiens et al., 2006) often utilize a calibration of > 55 mya based on the record of a supposed hylid ilium from the Paleocene of Itaboraí (Duellman and Trueb, 1986) for this node. However, this record is only a comment by Estes (1970) and Estes and Reig (1973) on a fossil that has never been described and apparently is not available in any collection. Also, note that Wiens et al. (2006) employed it for a more inclusive node, as they considered that this fossil could also be associated with Hemiphractidae—considered a subfamily of Hylidae at the time (Estes, 1970) and (Estes and Reig, 1973) associated those remains with Hylidae. Therefore, we utilized a much more conservative interpretation of the Hylidae fossil records and expanded the prior in our divergence-time analyses. Instead of a one-sided lower-bound prior, we included both a lower bound at 33.9 mya- *Hyla swanstoni* (Holman, 1968, 2003) and the discussed upper bound at 125 mya- remains of *Eurycephalella alcinae* and *Arariphrynus placidoi* (Báez et al., 2009). This change in prior, along with the fact that our taxonomic sampling was focused within *Dendropsophus*, likely caused the divergence in our study's estimated date of divergence from previous estimates.

Our estimated divergence occurred before the Andean uplift (40–24 mya) causing disjunction of the Amazonia and Atlantic Forest ~ 23 mya (Batalha-Filho et al., 2013). Although the Andean uplift was previously considered a barrier to amphibian dispersal (Ledo and Colli, 2017; Batalha-Filho et al., 2013), our results suggest that episodic movement between Amazonia and Atlantic Forest biomes within the last 70 million years is the best supported model for amphibian dispersal (Table S3). Our geographic results support an ancestral *Dendropsophus* range spanning Amazonia and the Atlantic Forest and subsequent range expansion and vicariant speciation of the eight species groups of *Dendropsophus* recognized here (Fig. 5). These diversification events occurred during the Andean uplift (Fig. 5), an event previously considered as a barrier to dispersal for amphibians due to lack of moist/wet conditions (Ledo and Colli, 2017). The dispersals of the different species groups of *Dendropsophus* that occurred during the Andean uplift included movement between Amazonia and the Atlantic Forest (Fig. 5). Instead of the previous view that the environmental niche changes caused by the Andean uplift provided a continuous barrier between the biomes of Amazonia and the Atlantic Forest (Ledo and Colli, 2017), our results present a dynamic picture in which a shifting barrier imposed by changing environmental conditions leads to alternating range expansion and vicariant speciation events within the ancestral population whose range spanned the dynamic area.

4.3. Oviposition site and mode-dependent diversification in Dendropsophus

Our study identified at least three independent transformations from aquatic to terrestrial egg deposition, which we tested for contribution to increasing the rate of diversification in this genus. A previous study of oviposition site evolution in *Dendropsophus* (Orrico et al., 2021) suggested at least three or four evolutionary transformations to terrestrial egg deposition. These transitions occurred: (1) in the most recent common ancestor of the *D. parviceps* group, (2) during the evolutionary history of the *D. leucophyllatus* group (as redefined here), and (3) either independently in the *D. decipiens* and *D. ruschii* groups (sensu Orrico

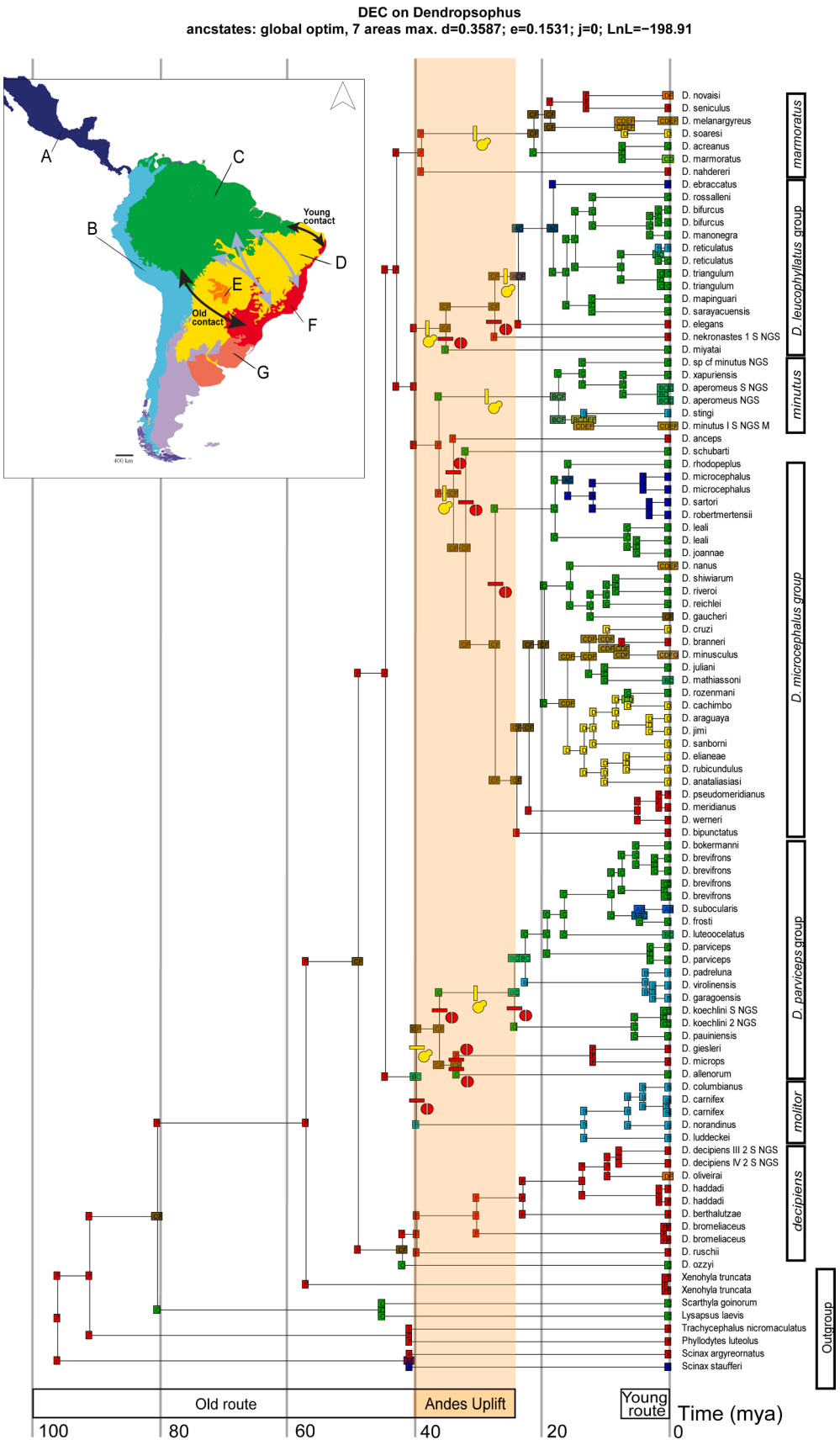

Fig. 5. Dispersal-Extinction-Cladogenesis map of the ancestral geographic area states of *Dendropsophus* from the unconstrained dispersal hypothesis analysis on the ASTRID tree (B). Letters correspond to the ecoregions defined in Fig. 1.

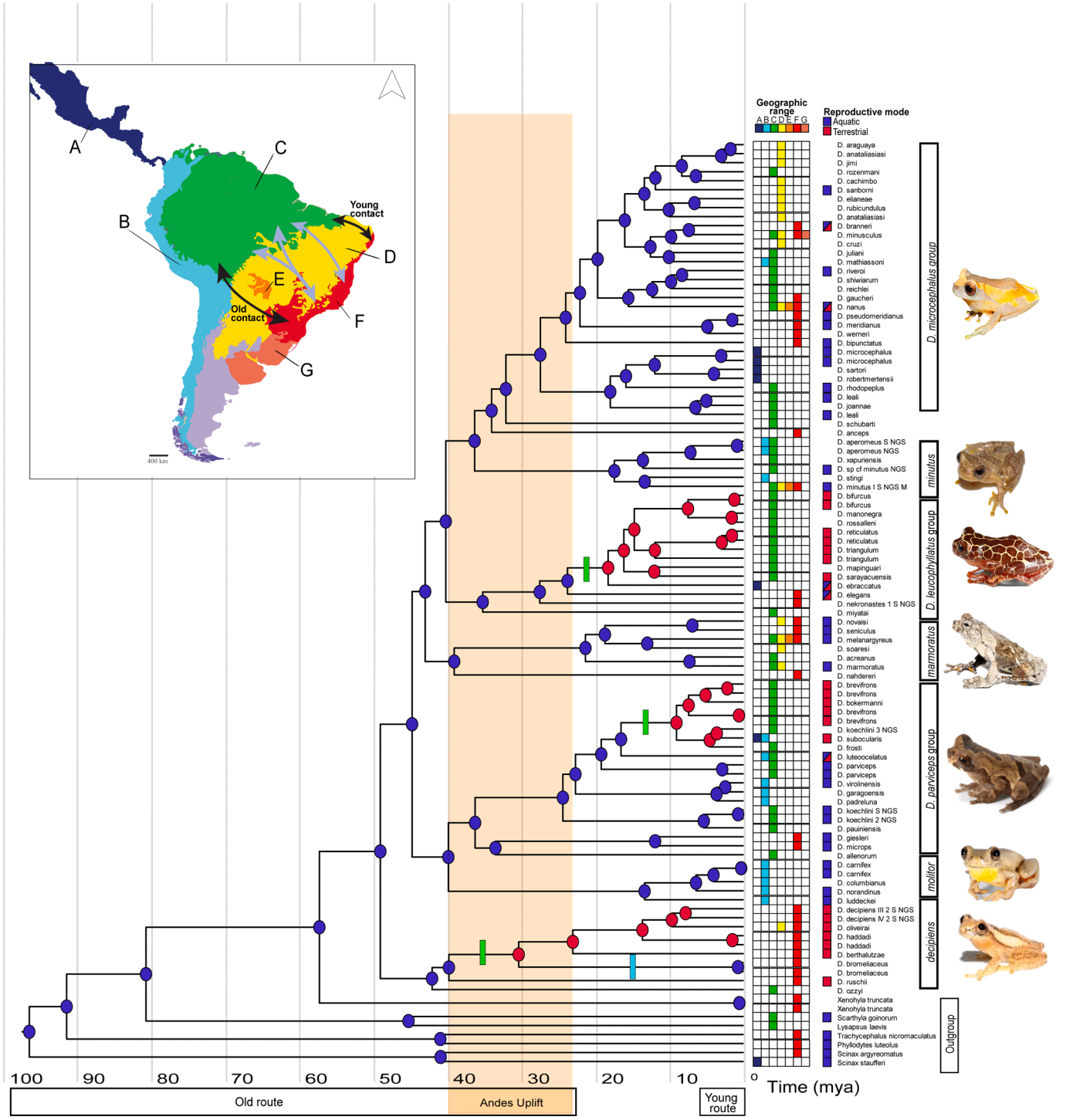

Fig. 6. Ancestral state reconstruction of oviposition sites in *Dendropsophus* and outgroups on the ASTRID tree (B). The estimated ancestral oviposition site state at each node is presented as aquatic (blue) and terrestrial (red) from the BiSSE model. Green ticks indicate a transformation to terrestrial and blue ticks to aquatic reproduction.

et al., 2021) or prior to the origin of *Dendropsophus* with a subsequent reversal to aquatic deposition in the most recent common ancestor of the clade including all species of *Dendropsophus* except those groups.

We provide support for at least three transformations from aquatic to terrestrial oviposition: (1) in the most recent common ancestor of the *Dendropsophus decipiens* group as redefined here, (2) in an internal clade of the *D. leucophyllatus* group, and (3) in an internal clade of the *D. parviceps* group (Fig. 6). The difference in the number of inferred transformation events possibly stems from the changes in the relationships of the former *D. ruschii* group obtained by Orrico et al. (2021) and our results. It should be considered that although the likelihood that the ancestral state for *Dendropsophus* was aquatic egg deposition is 90.91 % (Fig. 6), the oviposition site remains unknown for *D. ozzyi* (the sister taxon of the *D. decipiens* group) and the two species of *Xenohyla* (the sister taxon of *Dendropsophus*).

We did not find evidence for a correlation between egg deposition site and lineage accumulation rate or a correlation between evolution of egg deposition and geographic range as we had predicted. This result is

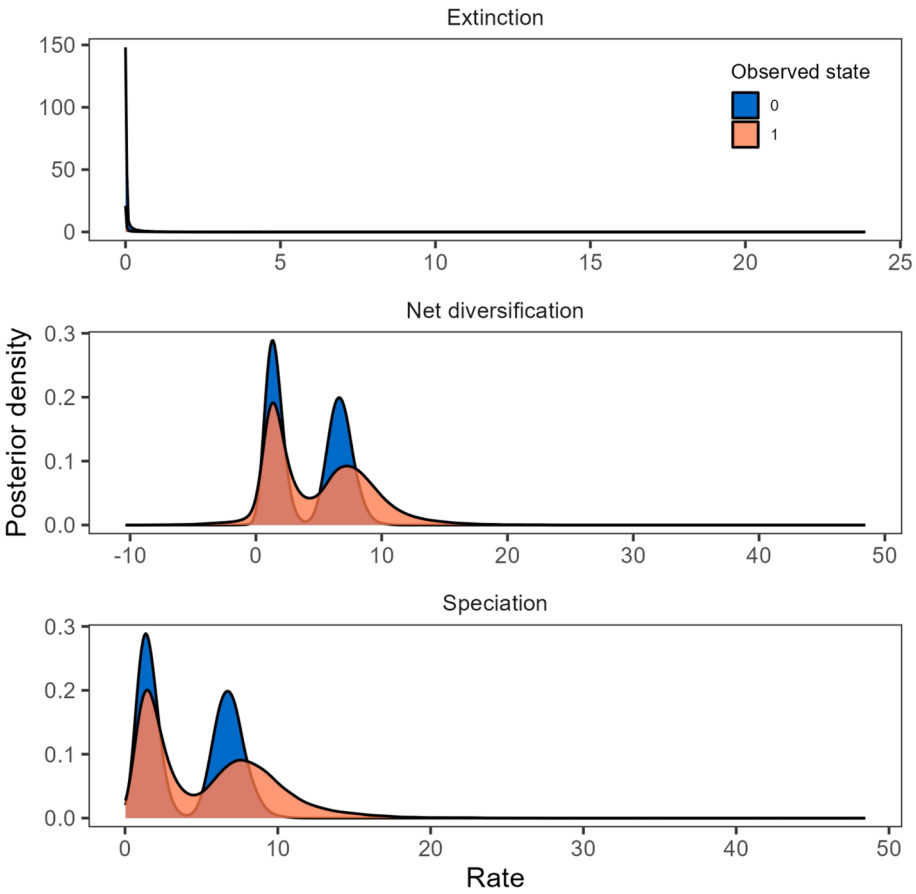

Fig. 7. Distribution of estimated extinction, net diversification, and lineage accumulation rates (in number of changes per unit of time) of taxa within *Dendropsophus* with aquatic egg deposition site (blue) and terrestrial egg deposition site (red) from an MCMC HiSSE analysis of 10,000 iterations on the ASTRID tree (B). There is no influence of egg deposition site on these rates; hidden traits are responsible for differences in diversification rates.

consistent with the estimated Pybus and Harvey's "gamma" statistic from our lineage accumulation analyses (gamma = 0.9603, p-value = 0.3369), suggesting that *Dendropsophus* diversified with constant rates. Only one of the three predicted transformations from aquatic to terrestrial egg deposition occurred during the Andean uplift (Fig. 6), but this transformation appears to have occurred while the lineage inhabited the Atlantic Forest (Fig. 5). It did not correlate with any of the many lineage-accumulation events in *Dendropsophus* during this period of time. The other egg-deposition site transformations instead occurred in the time between the two routes (old and young) predicted by Ledo and Colli (2017). While not correlated with inhabiting more than one geographic range (Fig. S11), perhaps these changes influenced smaller, population-level ability for survival and unconstrained population-level dispersal in *Dendropsophus* during this time.

4.4. Caveats

Our results are limited by the scale of the geographic ranges used in the analysis, the extremely incomplete fossil record for hylids, and the amount of information available on species oviposition sites. A significant relationship between dispersal and oviposition site could be hidden by these factors. For example, oviposition sites of species in the *D. microcephalus* group are undocumented, as are those of the two species of *Xenohyla*, the critical sister taxon of *Dendropsophus*. Additional dispersals and/or transformations might be masked by the current scale of the defined biomes. This deficiency of data stresses the importance of further collection of basic life-history data of *Dendropsophus* to improve knowledge on oviposition site evolution and better understand the factors driving lineage accumulation in this genus.

4.5. Conclusion

Overall, our phylogenomic data provide additional resolution and support for the evolutionary relationships among species of *Dendropsophus*. Our study provides insight into the biogeographic origin and expansion of the clade. Given that *Dendropsophus* is one of the most broadly ranging hylid genera in South America, our highly-supported tree provides an invaluable tool for future clade-specific and comparative studies investigating the evolution of biodiversity throughout these regions.

CRediT authorship contribution statement

Courtney Whitcher: Writing – review & editing, Writing – original draft, Visualization, Methodology, Investigation, Formal analysis, Data curation, Conceptualization. **Victor G.D. Orrico:** Writing – review & editing, Resources, Methodology, Investigation, Formal analysis, Data curation, Conceptualization. **Santiago Ron:** Writing – review & editing, Methodology, Investigation, Data curation, Conceptualization. **Mariana L. Lyra:** Validation, Resources, Investigation. **Carla S. Cassini:** Validation, Resources, Investigation. **Rodrigo B. Ferreira:** Validation, Resources, Investigation. **Daniel Y.M. Nakamura:** Validation, Resources, Investigation. **Pedro L.V. Peloso:** Writing – review & editing, Validation, Resources, Investigation. **Marco A. Rada:** Validation, Resources, Investigation. **Mauricio Rivera-Correa:** Validation, Resources, Investigation. **Marcelo J. Sturaro:** Validation, Resources, Investigation. **Paula H. Valdujo:** Validation, Resources, Investigation. **Célio F.B. Haddad:** Writing – review & editing, Validation, Resources, Investigation. **Taran Grant:** Conceptualization, Formal analysis, Resources,

Writing – review & editing, Methodology, Investigation, Data curation. **Julian Faivovich:** Resources, Writing – review & editing, Methodology, Investigation, Data curation, Conceptualization. **Alan Lemmon:** Writing – review & editing, Visualization, Validation, Resources, Methodology, Investigation, Formal analysis, Data curation, Conceptualization. **Emily Moriarty Lemmon:** Writing – review & editing, Visualization, Supervision, Resources.

Declaration of competing interest

The authors declare that they have no known competing financial interests or personal relationships that could have appeared to influence the work reported in this paper.

Acknowledgments

CW, ARL, and EML wish to thank Michelle Kortyna at Florida State University's Center for Anchored Phylogenomics for assistance with molecular data collection and analysis. This research was supported by funding from the U.S. National Science Foundation DEB#1120516, #1214325, #1314449, #1415545, and #1416134. PHV thanks Renato Recoder, Mauro Teixeira Jr, Agustin Camacho and Mara Silva for field companionship. This research was supported by the Brazilian Conselho Nacional de Desenvolvimento Científico e Tecnológico (CNPq Proc. 310467/2017-9, 431772/2018-5, 310256/2020-8, 314480/2021-8), the Fundação de Amparo à Pesquisa do Estado de São Paulo (FAPESP Proc. 2007/51956-6, 2007/57067-9, 2012/10000-5, 2013/50741-7, 2018/15425-0, 2021/10639-5), and Argentinean ANPCYT (PICT 346/2019, 59/2021), and CONICET (PIP 2800). Collection permits issued for specimens in this study include SISBIO/ICMBio 22511-1; 002/2006NP; 19754-2; 10126-1; 30309-3; 14398-1; 54666-1; 28190-1;13173-2; 13708-1; 13708-2; 19989-1; 759-2; 51522-1; 12920; 48034; 02001.001238/2007-52.

Appendix A. Supplementary material

Supplementary data to this article can be found online at https://doi.org/10.1016/j.ympev.2024.108275.

References

Antonelli, Alexandre & Zizka, Alexander & Antunes Carvalho, Fernanda & Scharn, Ruud & Bacon, Christine & Silvestro, Daniele & Condamine, Fabien. (2018). Amazonia is the primary source of Neotropical biodiversity. Proceedings of the National Academy of Sciences. 115. 201713819.

Araujo-Vieira, K., Blotto, B.L., Caramaschi, U., Haddad, C.F.B., Faivovich, J., Grant, T., 2019. A total evidence analysis of the phylogeny of hatchet-faced treefrogs (Anura: Hylidae: *Sphaenorhynchus*). Cladistics 35, 469–486. https://doi.org/10.1111/cla.12367.

Araujo-Vieira, K., Lourenço, A.C.C., Lacerda, J.V.A., Lyra, M.L., Blotto, B.L., Ron, S.R., Baldo, D., Pereyra, M.O., Suárez-Mayorga, Á.M., Baêta, D., Ferreira, R.B., Barrio-Amorós, C.L., Borteiro, C., Brandão, R.A., Brasileiro, C.A., Donnelly, M.A., Dubeux, M.J.M., Köhler, J., Kolenc, F., Fortes Leite, F.S., Maciel, N.M., Nunes, I., Orrico, V.G.D., Peloso, P., Pezzuti, T.L., Reichle, S., Rojas-Runjaic, F.J.M., Da Silva, H.R., Sturaro, M.J., Langone, J.A., Garcia, P.C.A., Rodrigues, M.T., Frost, D.R., Wheeler, W.C., Grant, T., Pombal, J.P., Haddad, C.F.B., Faivovich, J., 2023. Treefrog diversity in the Neotropics: Phylogenetic relationships of Scinaxini (Anura: Hylidae: Hylinae). South American Journal of Herpetology 27, 1–143. https://doi.org/10.2994/SAJH-D-22-00038.1.

Arias-Cárdenas, A., Barrientos, L.S., Pardo-Diaz, C., Paz, A., Crawford, A.J., Salazar, C., 2024. Taxonomic inflation and a reconsideration of lineage accumulation in the Andes: the case of the high-elevation tree frog *Dendropsophus molitor* (Anura: Hylidae). Zool. J. Linn. Soc. 200 (3), 763–775.

Báez, A.M., Moura, G.J., Gómez, R.O., 2009. Anurans from the Lower Cretaceous Crato Formation of northeastern Brazil: implications for the early divergence of Neobatrachians. Cretac. Res. 30 (4), 829–846.

Banker, S.E., Lemmon, A.R., Hassinger, A.B., Dye, M., Holland, S.D., Kortyna, M.L., Ospina, O.E., Ralicki, H., Lemmon, E.M., 2020. Hierarchical hybrid enrichment: multitiered genomic data collection across evolutionary scales, with application to Chorus Frogs (*Pseudacris*). Syst. Biol. 69 (4), 756–773.

Barrow, L.N., Lemmon, A.R., Lemmon, E.M.L., 2018. Targeted sampling and target capture: assessing phylogeographic concordance with genome-wide data. Syst. Biol. 67, 979–996.

Batalha-Filho, H., Fjeldså, J., Fabre, P.-H., Miyaki, C.Y., 2013. Connections between the Atlantic and the Amazonian forest avifaunas represent distinct historical events. J. Ornithol. 154, 41–50.

Blotto, B.L., Lyra, M.L., Cardoso, M.C.S., Rodrigues, M.T., R. Dias, I., Marciano-Jr, E., Dal Vechio, F., Orrico, V.G.D., Brandão, R.A., Lopes de Assis, C., Lantyer-Silva, A.S.F., Rutherford, M.G., Gagliardi-Urrutia, G., Solé, M., Baldo, D., Nunes, I., Cajade, R., Torres, A., Grant, T., Jungfer, K., Silva, H.R., Haddad, C.F.B., Faivovich, J., 2021. The phylogeny of the casque-headed treefrogs (Hylidae: Hylinae: Lophyohylini). Cladistics 37, 36–72. https://doi.org/10.1111/cla.12409.

Bokermann, W.C.A., 1963. Girinos de anfíbios brasileiros (Amphibia - Salientia). Anais da Academia Brasileira de Ciências 35 (3), 465–474.

Bokermann, W.C.A., 1964. Dos nuevas especies de *Hyla* de Rondonia, Brasil (Amphibia, Salientia, Hylidae). Neotropica 10 (31), 2–6.

Bremer, K., 1988. The limits of amino acid sequence data in angiosperm phylogenetic reconstruction. Evolution 42, 795–803. https://doi.org/10.1111/j.1558-5646.1988.tb02497.x.

Caminer, M.A., Milá, B., Jansen, M., Fouquet, A., Venegas, P.J., Chávez, G., Lougheed, S. C., Ron, S.R., 2017. Systematics of the *Dendropsophus leucophyllatus* species complex (Anura: Hylidae): cryptic diversity and the description of two new species. PLoS One 12, e0171785.

Crump M.L. (1974). Reproductive strategies in a tropical anuran community. Miscellaneous Publication, Museum of Natural History, University of Kansas **61**, 1–68.

de Sá, F.P., Haddad, C.F.B., Gray, M.M., Verdade, V.K., Thomé, M.T.C., Rodrigues, M.T., Zamudio, K.R., 2020. Male-male competition and repeated evolution of terrestrial breeding in Atlantic Coastal Forest frogs. Evolution 74 (2), 459–475.

Dolinay, M., Nečas, T., Zimkus, B.M., Schmitz, A., Fokam, E.B., Lemmon, E.M., Lemmon, A.R., Gvoždík, V., 2021. Gene flow in phylogenomics: sequence capture resolves species limits and biogeography of Afromontane forest endemic frogs from the Cameroon Highlands. Mol. Phylogenet. Evol. 163, 107258.

dos Reis M., Yang Z. (2019) Bayesian molecular clock dating using genome-scale datasets. In: Anisimova M. (eds) Evolutionary Genomics. Methods in Molecular Biology, vol 1910. Humana, New York, NY.

Duellman, W. E., Crump, M. L. (1974). Speciation in frogs of the *Hyla parviceps* group in the upper Amazon Basin. Occasional Papers of the Museum of Natural History of the University of Kansas 23, 1-40.

Duellman W.E. (1978). The biology of an equatorial herpetofauna in Amazonian Ecuador. Miscellaneous Publications of the Museum of Natural History of the University of Kansas 65, 1-352.

Duellman, W. E. (2001). Hylid frogs of Middle America. Society for the Study of Amphibians and Reptiles, Ithica, New York, U.S.A., 1158 pp.

Duellman, W.E., Trueb, L., 1986. Biology of Amphibians. McGraw-Hill, New York.

Dupin, J., Matzke, N.J., Sarkinen, T., Knapp, S., Olmstead, R., Bohs, L., Smith, S., 2016. Bayesian estimation of the global biogeographic history of the Solanaceae. J. Biogeogr. 44 (4), 887–899.

Edwards, A., 1972. Likelihood. Cambridge University Press, Cambridge.

Elmer, K.R., Bonett, R.M., Wake, D.B., 2013. Early Miocene origin and cryptic diversification of South American salamanders. BMC Evol. Biol. 13, 59. https://doi.org/10.1186/1471-2148-13-59.

Estes, R., 1970. Origin of the recent North American lower vertebrate fauna: An inquiry into the fossil record. Forma et Functio 3, 139163.

Estes, R., Reig, O., 1973. The early fossil record of frogs: A review of the evidence. In: Vial, J. (Ed.), Evolutionary Biology of the Anurans. University of Missouri Press, Columbia, Missouri, USA, p. 1163.

Faivovich, J., Haddad, C.F.B., Garcia, P.C.A., Frost, D.R., Campbell, J.A., Wheeler, W.C., 2005. Systematic review of the frog family Hylidae, with special reference to Hylinae: phylogenetic analysis and taxonomic revision. Bull. Am. Mus. Nat. Hist. 294, 1–240.

Ferrão, M., Moravec, J., Hanken, J., Lima, A.P., 2020. A new species of *Dendropsophus* (Anura, Hylidae) from southwestern Amazonia with a green bilobate vocal sac. ZooKeys 942, 77.

Fouquet, A., Santana Cassini, C., Fernando Baptista Haddad, C., Pech, N., & Trefaut Rodrigues, M. (2014). Species delimitation, patterns of diversification and historical biogeography of the Neotropical frog genus *Adenomera* (Anura, Leptodactylidae). Journal of Biogeography, 41(5), 855–870.

Fouquet, A., Noonan, B.P., Blanc, C.P., Orrico, V.G.D., 2011. Phylogenetic position of *Dendropsophus gaucheri* (Lescure and Marty 2000) highlights the need for an in-depth investigation of the phylogenetic relationships of *Dendropsophus* (Anura: Hylidae). Zootaxa 3035, 59–67.

Frost, D.R., 2024. Amphibian species of the world: an online reference. Version 6.2 (29 June 2024). Electronic Database accessible at http://research.amnh.org/herpetology/amphibia/index.php. American Museum of Natural History, New York, USA. https://doi.org/10.5531/db.vz.0001.

Gehara, M., Crawford, A.J., Orrico, V.G.D., Rodríguez, A., Lötters, S., et al., 2014. High levels of diversity uncovered in a widespread nominal taxon: continental phylogeography of the neotropical tree frog *Dendropsophus minutus*. PLoS One 9 (9), e103958.

Goloboff, P.A., Catalano, S.A., 2016. TNT version 1.5, including a full implementation of phylogenetic morphometrics. Cladistics 32 (3), 221–238.

Goloboff, P.A., Farris, J.S., Nixon, K.C., 2008. TNT, a free program for phylogenetic analysis. Cladistics 24 (5), 774–786.

Goodman, M., Olson, C.B., Beeber, J.E., Czelusniak, J., 1982. New perspectives in the molecular biological analysis of mammalian phylogeny. Acta Zoologica Fennica 169, 19–35.

Hamilton, C.A., Lemmon, A.R., Moriarty Lemmon, E., Bond, J.E., 2016. Expanding Anchored Hybrid Enrichment to resolve both deep and shallow relationships within the spider Tree of Life. BMC Evol. Biol. 16, 212.
Hedges, S.B., Marin, J., Suleski, M., Paymer, M., Kumar, S., 2015. Tree of life reveals clock-like speciation and diversification. Mol. Biol. Evol. 32 (4), 835–845.
Heinicke, M.P., Duellman, W.E., Hedges, S.B., 2007. Major Caribbean and Central American frog faunas originated by ancient oceanic dispersal. Proc. Natl. Acad. Sci. 104 (24), 10092–10097.
Hime, P.M., Lemmon, A.R., Lemmon, E.C.M., Prendini, E., Brown, J.M., Thomson, R.C., Kratovil, J.D., Noonan, B.P., Pyron, R.A., Peloso, P.L.V., Kortyna, M.L., Keogh, J.S., Donnellan, S.C., Mueller, R.L., Raxworthy, C.J., Kunte, K., Ron, S.R., Das, S., Gaitonde, N., Weisrock, D.W., 2021. Phylogenomics reveals ancient gene tree discordance in the amphibian tree of life. Syst. Biol. 70 (1), 49–66.
Hoang, D.T., Chernomor, O., Von Haeseler, A., Minh, B.Q., Vinh, L.S., 2018. UFBoot2: improving the ultrafast bootstrap approximation. Mol. Biol. Evol. 35 (2), 518–522.
Höhna, S., Heath, T.A., Boussau, B., Landis, M.J., Ronquist, F., Huelsenbeck, J.P., 2014. Probabilistic graphical model representation in phylogenetics. Syst. Biol. 63, 753–771.
Höhna, S., Landis, M.J., Heath, T.A., Boussau, B., Lartillot, N., Moore, B.R., Huelsenbeck, J.P., Ronquist, F., 2016. RevBayes: Bayesian phylogenetic inference using graphical models and an interactive model-specification language. Syst. Biol. 65 (4), 726–736.
Holman, J.A., 2003. Fossil frogs and toads of North America. Indiana University Press, Bloomington.
Holman, J.A. (1968). Lower Oligocene amphibians from Saskatchewan. Florida Academy of Sciences, Quarterly Journal 31:273-289.
Hoorn, C., Wesselingh, F.P., ter Steege, H., Bermudez, M.A., Mora, A., Sevink, J., Sanmartín, I., Sanchez-Meseguer, A., Anderson, C.L., Figueiredo, J.P., Jaramillo, C., Riff, D., Negri, F.R., Hooghiemstra, H., Lundberg, J., Stadler, T., Särkinen, T., Antonelli, A., 2010. Amazonia through time: Andean uplift, climate change, landscape evolution, and biodiversity. Science (New York, N.Y.) 330 (6006), 927–931.
Jungfer, K.-H., Reichle, S., Piskurek, O., 2010. Description of a new cryptic southwestern Amazonian species of leaf-gluing treefrog, genus *Dendropsophus* (Amphibia: Anura: Hylidae). Salamandra 46, 204–213.
Kalyaanamoorthy, S., Minh, B.Q., Wong, T.K., Von Haeseler, A., Jermiin, L.S., 2017. ModelFinder: fast model selection for accurate phylogenetic estimates. Nat. Methods 14 (6), 587–589.
Katoh, K., Standley, D.M., 2013. MAFFT multiple sequence alignment software version 7: improvements in performance and usability. Mol. Biol. Evol. 30, 772–780.
Kearse, M., Moir, R., Wilson, A., Stones-Havas, S., Cheung, M., Sturrock, S., Buxton, S., Cooper, A., Markowitz, S., Duran, C., et al., 2012. Geneious basic: an integrated and extendable desktop software platform for the organization and analysis of sequence data. Bioinformatics 28, 1647–1649.
Köhler, J., Lötters, S., 2001. A new species of minute *Hyla* from the southwestern Amazon Basin (Amphibia, Anura, Hylidae). Stud. Neotropical Fauna Environ. 36 (2), 105–112. https://doi.org/10.1076/snfe.36.2.105.2135.
Ledo, R.M.D., Colli, G.R., 2017. The historical connections between the Amazon and the Atlantic Forest revisited. J. Biogeogr. 44, 2551–2563.
Lemmon, A.R., Emme, S.A., Lemmon, E.M., 2012. Anchored hybrid enrichment for massively high-throughput phylogenomics. Syst. Biol. 61 (5), 727–744.
Lutz, B., 1973. Brazilian Species of Hyla. Austin, University of Texas Press; xix +, p. 260–p.
Machado, D.J., Marques, F.P., de, L., Jiménez-Ferbans, L., Grant, T., 2022. An empirical test of the relationship between the bootstrap and likelihood ratio support in maximum likelihood phylogenetic analysis. Cladistics 38, 392–401. https://doi.org/10.1111/cla.12496.
Mageski, M., Silva-Soares, T., & Ferreira, R. B. (2014). Hábito bromelígena de Dendropsophus haddadi (Anura: Hylidae) em ambiente de Mata Atlântica no sudeste do Brasil. Boletim do Museu de Biologia Mello Leitão, 34, 97-100.
Magnusson, W.E., Hero, J.-M., 1991. Predation and the evolution of complex oviposition behaviour in Amazon rainforest frogs. Oecologia 86 (3), 310–318.
Matzke, N.J., 2013. Probabilistic historical biogeography: new models for founder-event lineage accumulation, imperfect detection, and fossils allow improved accuracy and model-testing. Front. Biogeogr. 5 (4), 242–248.
Matzke, Nicholas J. (2016). "Stochastic mapping under biogeographical models." PhyloWiki BioGeoBEARS website, 2016, http://phylo.wikidot.com/biogeobears#stochastic_mapping.
Melo-Sampaio, P. R. (2023). On the taxonomic status of *Dendropsophus koechlini* (Duellman & Trueb, 1989). Journal of Vertebrate Biology, 72(23022), 23022-1.
Meyer, M., & Kircher, M. (2010). Illumina sequencing library preparation for highly multiplexed target capture and sequencing. Cold Spring Harbor protocols, 2010(6), pdb.prot5448.
Minh, B.Q., Nguyen, M.A.T., Von Haeseler, A., 2013. Ultrafast approximation for phylogenetic bootstrap. Mol. Biol. Evol. 30 (5), 1188–1195.
Minh, B.Q., Schmidt, H.A., Chernomor, O., Schrempf, D., Woodhams, M.D., Von Haeseler, A., Lanfear, R., 2020. IQ-TREE 2: new models and efficient methods for phylogenetic inference in the genomic era. Mol. Biol. Evol. 37 (5), 1530–1534.
Oliveira, R.F.D., Magalhães, F.D.M., Teixeira, B.F.D.V., Moura, G.J.B.D., Porto, C.R., Guimarães, F.P.B.B., Giaretta, A.A., Tinôco, M.S., 2021. A new species of the *Dendropsophus decipiens* Group (Anura: Hylidae) from Northeastern Brazil. PLoS ONE 16, e0248112. https://doi.org/10.1371/journal.pone.0248112.
Oliveira, P.R., Oliveira, P., Barreto, A.M., Suguio, K., 1999. Late Pleistocene/Holocene climatic and vegetational history of the Brazilian caatinga: the fossil dunes of the middle São Francisco River. Palaeogeogr. Palaeoclimatol. Palaeoecol. 152, 319–337.
Orrico, V., Grant, T., Faivovich, F., Rivera-Correa, M., Rada, M., Lyra, M., Cassini, C., Valdujo, P., Schargel, W., Machado, D., Wheeler, W., Barrio-Amoros, C., Loebmann, D., Moravec, J., Zina, J., Sole, M., Sturaro, M., Peloso, P., Suarez, P., Haddad, C., 2021. The phylogeny of Dendropsophini (Anura: Hylidae: Hylinae). Cladistics 37, 73–105.
Padial, J.M., Grant, T., Frost, D.R., 2014. Molecular systematics of terraranas (Anura: Brachycephaloidea) with an assessment of the effects of alignment and optimality criteria. Zootaxa 3825, 1–132. https://doi.org/10.11646/zootaxa.3825.1.1.
Paradis, E., Schliep, K., 2019. ape 5.0: an environment for modern phylogenetics and evolutionary analyses in R. Bioinformatics 35, 526–528.
Peloso, P.L.V., Orrico, V.G.D., Haddad, C.F.B., Lima-Filho, G.R., Sturaro, M.J., 2016. A new species of clown tree frog, *Dendropsophus leucophyllatus* species group, from Amazonia (Anura, Hylidae). South American Journal of Herpetology 11, 66–80. https://doi.org/10.2994/SAJH-D-16-00003.1.
Pirani, R., Peloso, P., Prado, J., Polo, É., Knowles, L., Ron, S., Rodrigues, M., Sturaro, M., Werneck, F., 2020. Diversification history of clown tree frogs in neotropical rainforests (Anura, Hylidae, *Dendropsophus leucophyllatus* group). Mol. Phylogenet. Evol. 150, 106877.
Por, F. D. (1992). Sooretama: The Atlantic Rain Forest of Brazil. The Hague: SPB Academic Publishing. Netherlands.
Portik, D.M., Streicher, J.W., Wiens, J.J., 2023. Frog phylogeny: a time-calibrated, species-level tree based on hundreds of loci and 5,242 species. Mol. Phylogenet. Evol. 188, 107907.
Prum, R.O., Berv, J.S., Dornburg, A., Field, D.J., Townsend, J.P., Lemmon, E.M., Lemmon, A.R., 2015. A comprehensive phylogeny of birds (Aves) using targeted next-generation DNA sequencing. Nature 526 (7574), 569–573.
Pybus, O.G., Harvey, P.H., 2000. Testing macro-evolutionary models using incomplete molecular phylogenies. Proc. R. Soc. B Biol. Sci. 267 (1459), 2267–2272.
Pyron, A., 2014. Biogeographic analysis reveals ancient continental vicariance and recent oceanic dispersal in amphibians. Syst. Biol. 63 (5), 779–797.
R Core Team. (2023). R: A language and environment for statistical computing. R Foundation for Statistical Computing, Vienna, Austria. https://www.R-project.org/.
Rambaut, A. (2009). FigTree. Tree figure drawing tool. http://tree.bio.ed.ac.uk/software/figtree/.
Ree, R.H., Smith, S.A., 2008. Maximum likelihood inference of geographic range evolution by dispersal, local extinction, and cladogenesis. Syst. Biol. 57 (1), 4–14.
Revell, L.J., 2024. Phytools 2.0: an updated R ecosystem for phylogenetic comparative methods (and other things). PeerJ 12, e16505.
Rivadeneira, C.D., Venegas, P.J., Ron, S.R., 2018. Species limits within the widespread Amazonian treefrog *Dendropsophus parviceps* with descriptions of two new species (Anura, Hylidae). ZooKeys 726, 25.
Rivera-Correa, M., Orrico, V.G.D., 2013. Description and phylogenetic relationships of a new species of treefrog of the *Dendropsophus leucophyllatus* group (Anura: Hylidae) from Amazon Basin of Colombia and with an exceptional color pattern. Zootaxa 3680, 447–460.
Robinson, D.F., Foulds, L.R., 1981. Comparison of phylogenetic trees. Math. Biosci. 53 (1–2), 131–147.
Rodríguez Tribaldos, V., White, N.J., Roberts, G.G., Hoggard, M.J., 2017. Spatial and temporal uplift history of South America from calibrated drainage analysis. Geochem. Geophys. Geosyst. 18 (6), 2321–2353.
Rohrmann, A., Sachse, D., Mulch, A., Pingel, H., Tofelde, S., Alonso, R.N., Strecker, M.R., 2016. Miocene orographic uplift forces rapid hydrological change in the southern central Andes. Sci. Rep. 6 (1), 35678.
Rokyta, D.R., Lemmon, A.R., Margres, M.J., Arnow, K., 2012. The venom-gland transcriptome of the eastern diamondback rattlesnake (*Crotalus adamanteus*). BMC Genomics 13, 312.
Sanchíz, B. (1998). Handbuch der Palaoherpetologie. Part 4: Salientia. Munchen: Verlag Dr. Friedrich Pfeil, 275 pp.
Santos, J.C., Coloma, L.A., Summers, K., Caldwell, J.P., Ree, R., et al., 2009. Amazonian amphibian diversity is primarily derived from late Miocene Andean lineages. PLoS Biol. 7 (3), e1000056.
Schiesari, L. C., de C. Rossa-Feres, D., Menin, M., Hödl, W. (2022). Tadpoles of central Amazonia (Amphibia: Anura). Zootaxa 5223: 1–149.
Seger, K.R., da Veiga Teixeira, B.F., Annibale, F.S., Rossa-Feres, D.d.C., Lima, A.P., Andrade, G.V., Giaretta, A.A., Lourenço, L.B. (2021). Five independent lineages revealed by integrative taxonomy in the *Dendropsophus nanus–Dendropsophus walfordi* species complex. Diversity, 13, 522.
Smith, M.R. (2020). TreeDist: Distances between phylogenetic trees. R package version 2.7.0. Comprehensive R Archive Network.
Stamatakis, A., 2006. RAxML-VI-HPC: maximum likelihood-based phylogenetic analyses with thousands of taxa and mixed models. Bioinformatics 22, 2688–2690.
Touchon, J.C., 2012. A treefrog with reproductive mode plasticity reveals a changing balance of selection for nonaquatic egg laying. Am. Nat. 180 (6), 733–743.
Touchon, J.C., Warkentin, K.M., 2008. Reproductive mode plasticity: aquatic and terrestrial oviposition in a treefrog. Proc. Natl. Acad. Sci. 105 (21), 7495–7499.
Touchon, J.C., Worley, J.L., 2015. Oviposition site choice under conflicting risks demonstrates that aquatic predators drive terrestrial egg-laying. Proc. R. Soc. B Biol. Sci. 282 (1808), 20150376.
Vachaspati, P., Warnow, T., 2015. ASTRID: accurate species trees from internode distances. BMC Genomics 16 (Suppl 10), S3.
Vasconcelos, T.S., da Silva, F.R., dos Santos, T.G., Prado, V.H.M., Provete, D.B. (2019). An introduction to the biogeography of South American Anurans. In: Biogeographic Patterns of South American Anurans. Springer, Cham.
Weygoldt, P., Peixoto, O.L., 1987. *Hyla ruschii* n. sp., a new frog from the Atlantic Forest domain in the state of Espirito Santo, Brazil (Amphibia, Hylidae). Stud. Neotropical Fauna Environ. 22 (4), 237–247.

Wheeler, W.C., Lucaroni, N., Hong, L., Crowley, L.M., Varón, A., 2015. POY version 5: phylogenetic analysis using dynamic homologies under multiple optimality criteria. Cladistics 31 (2), 189–196.

Wickham, H., 2023. Stringr: simple, consistent wrappers for common string operations. R Package Version 1 (5), 1. https://CRAN.R-project.org/package=stringr.

Wiens, J., Graham, C., Moen, D., Smith, S., Reeder, T., 2006. Evolutionary and ecological causes of the latitudinal diversity gradient in Hylid frogs: treefrog trees unearth the roots of high tropical diversity. Am. Nat. 168 (5), 579–596.

Wogel, H., Abrunhosa, P.A., Pombal Jr., J.P., 2000. Girinos de cinco espécies do sudeste do Brasil (Amphibia: Hylidae. Leptodactylidae, Microhylidae). Bol. Mus. Nacl Nova Sér. Zool. 427, 1–16.

Zamudio, K.R., Bell, R.C., Nali, R.C., Haddad, C.F.B., Prado, C.P.A., 2016. Polyandry, predation, and the evolution of frog reproductive modes. Am. Nat. 188 (Suppl 1), S41–S61.